



**TECHNICAL UNIVERSITY  
of GABROVO**

**Faculty of  
MECHANICAL AND PRECISION  
ENGINEERING**

Assoc. Prof. TSANKA DIMITROVA DIKOVA PhD,  
MSc, Mech. Eng.

**PROPERTIES OF ADDITIVELY MANUFACTURED  
DENTAL MATERIALS**

**ABSTRACT**

of dissertation for awarding a scientific degree

**"DOCTOR OF SCIENCE"**

Professional Area:

**5.6. Materials and Materials Science**

Scientific specialty:

**Material science and technology of (machine-building) materials**

**Scientific reviewers:**

Prof. DSc Eng. Jordan Todorov Maximov

Prof. D-r Eng. Stoyko Atanasov Gyurov

Prof. D-r Eng. Lyubomir Vankov Dimitrov

GABROVO, BULGARIA  
2019

The dissertation is written on 260 pages and illustrated with 23 tables and 162 figures. The references consist of 359 titles, 20 of which in Cyrillic and 339 in Latin. The numbering of the figures, tables and formulas in the abstract is the same like in the dissertation.

The dissertation is admitted to defense at a Scientific Jury of an extended departmental council of the Department of Mechanical Engineering Equipment and Technologies, Faculty of Mechanical and Precision Engineering at the Technical University of Gabrovo on 12 April 2019.

The public defense of DSc thesis will be held at an open session of the Scientific Jury on 10 July 2019 at 1.30 pm in the Conference hall at the Rectorate building of TU – Gabrovo.

The defense materials are available at the Science Department and on the website of TU - Gabrovo.

# CONTENT

	Page
Abbreviations used .....	4
INTRODUCTION .....	5
AIM AND TASKS OF THE RESEARCH .....	8
<i>SECOND CHAPTER: METHODS OF THE RESEARCH</i>	9
RESULTS	
<i>THIRD CHAPTER: ACCURACY AND ROUGHNESS OF DENTAL POLYMERS AND ALLOYS, MANUFACTURED BY ADDITIVE TECHNOLOGIES</i>	21
<i>FOURTH CHAPTER: MICROSTRUCTURE AND HARDNESS OF DENTAL ALLOYS, MANUFACTURED BY ADDITIVE TECHNOLOGIES</i>	38
<i>FIFTH CHAPTER: STRENGTH PROPERTIES AND TRIBO-CORROSION OF DENTAL ALLOYS, MANUFACTURED BY ADDITIVE TECHNOLOGIES</i>	45
<i>SIXTH CHAPTER: ADDITIVE TECHNOLOGIES IN PRODUCTION OF DENTAL CONSTRUCTIONS .....</i>	73
CONCLUSION .....	80
CONTRIBUTIONS .....	81
PUBLICATIONS ON DISSERTATION .....	85

## **ABBREVIATIONS USED**

ABS – Acrylonitrile Butadiene Styrene  
ADA - American Dental Association  
ANSI - American National Standard Institute  
ASTM - American Society for Testing and Materials  
AT – Additive Technologies  
BCC – Body Centered Cubic (lattice)  
CAD/CAM - Computer Aided Design/Computer Aided Manufacturing  
CAE - Computer Aided Engineering  
CTE – Coefficient of Thermal Expansion  
DLP – Digital Light Projection  
DLSP – Direct Laser Sintering of Metals  
EDX – Electro Dispersive X-ray  
FDM – Fuse Deposition Modeling  
FOS - Factor Of Safety  
FPD – Fixed Partial Dentures  
HCP – Hexagonal Close Packed (lattice)  
HTT – Hard Teeth Tissues  
IJP – Ink-Jet Printing  
ISO – International Standard Organization  
MAD/MAM - Manual Aided Design /Manual Aided Manufacturing  
MJM – Multi-Jet Modelling  
MPB – Melted Pool Boundaries  
OM – Optical Microscopy  
PLA - Polylactic Acid  
PMMA – Poly-Methyl Methacrylate  
SEBM – Selective Electron Beam Melting  
SEM – Scanning Electron Microscopy  
SLA - Stereolithography  
SLM – Selective Laser Melting  
SLS – Selective Laser Sintering

## INTRODUCTION

The first technologies for producing of details, which arose at the dawn of the humanity, are based on the principle of material removal. With the development of the technical progress, nowadays the modern nanotechnologies are being reached, in which the objects are built by self-organization or self-assembling of the building blocks. The present research deals with a new group of technologies, which arose in the late 80s of the last century, in which the details are manufactured layer by layer by polymerization, melting or sintering - the so called “additive technologies” (AT). The various technological processes, that are used, allow working with the almost a whole range of known materials. The capabilities of embedding the production equipment into the CAM module of the modern CAD/CAM systems and the use of specialized software, compatible with other software products, allow efficient and high-precision fabrication of customized details with a dense or porous structure and a predefined roughness. All these advantages make the additive technologies a successful alternative to the classical ones in the production of different types of constructions in dental and general medicine.

Several types of AT are mainly applied in dentistry: stereolithography (SLA) with laser or digital light projection (DLP); fused deposition modelling (FDM); inkjet printing (IJP), multi-jet printing; selective electron beam melting (SEBM); selective laser sintering (SLS) and selective laser melting (SLM). The group of AT characterises with: 1) higher accuracy and higher surface roughness of the details comparing to the conventional; 2) deformations of the constructions, depending on the process type; 3) obtaining a dense or porous structure with a corresponding selection of the technological parameters and 4) a specific fine-grained microstructure in SLM and SEBM of metals and alloys, resulting in increased mechanical properties. It should be noted that each 3D printing equipment works with a material or group of materials specific to it, and that the type and purpose of the dental construction determine the material and technology, which will be used for its production. The combination of many technological processes with the wide variety of materials

allows the production of dental constructions with different purposes for all areas of dental medicine - surgery, oral implantology, conservative dentistry, orthodontics and prosthetic dentistry. There are three approaches for application of AT in manufacturing of fixed partial dentures (FPDs): 1) for fabrication of temporary crowns and bridges of polymers/composites; 2) in casting of permanent FPDs or frameworks for them from dental alloys with 3D printed models and 3) direct production of metallic infrastructure or ceramic restoration from the virtual model by SLM, SEBM or SLS.

Since the additive technologies are highly effective in terms of productivity and quality of production, they are now rapidly finding their implementation into the dental clinics and laboratories. This process is supported by the rapid development of the information and communication technologies on a global scale.

Due to the extremely intensive development and improvement of the technological processes, equipment and materials, as well as their implementation into practice almost immediately after their development, a great number of unresolved issues, related to the quality of the manufactured details, remain.

The wide variety of constructions, used for treatment in dentistry, requires not only standardized specimens and methodologies to be used in investigations, but also to develop new methods for testing of real dental restorations in environments and conditions as close as possible to the actual ones.

All these reasons require constant research on the geometrical characteristics, physical and mechanical properties of the constructions, fabricated of different materials through additive technologies.

*I dedicate the present work to my parents - my mother Radka and my father Dimitar Dimitrovs with all my filial love, respect and gratitude!*

## **AIM AND TASKS OF THE RESEARCH**

### **AIM**

To investigate the properties of additively manufactured dental materials and to establish the conditions for their applicability in dental medicine.

### **TASKS**

1. To examine the accuracy and surface roughness of dental polymers and alloys manufactured by additive technologies.
  - 1.1. To investigate dental polymers produced by various 3D printing processes – DLP stereolithography, laser stereolithography and fused deposition modeling;
  - 1.2. To investigate dental alloys, cast with 3D printed patterns;
  - 1.3. To investigate Co-Cr dental alloys, fabricated by selective laser melting.
2. To investigate microstructure and hardness of dental alloys, manufactured by additive technologies.
3. To investigate strength properties and tribo-corrosion of dental alloys, fabricated by additive technologies – cast with 3D printed patterns and manufactured by SLM.
  - 3.1. To investigate strength characteristics;
  - 3.2. To investigate adhesion strength of porcelain and composite coatings;
  - 3.3. To investigate bending strength;
  - 3.4. To investigate tribo-corrosion properties.
4. To develop improved additive technologies for production of dental constructions.
  - 4.1. Technological process for fabricating of temporary crowns and bridges by stereolithography;
  - 4.2. Technological process for manufacturing of fixed partial dentures from dental alloys by casting with 3D printed patterns;
  - 4.3. Technological process for production of fixed partial dentures of Co-Cr dental alloys by SLM.

## SECOND CHAPTER

### METHODS OF THE RESEARCH

#### 2.1. SAMPLES AND FABRICATING METHODS

##### 2.1.1. Samples types

Three groups of samples were used in the present study: 1) cubes with dimensions 5 mm x 5 mm x 5 mm (Fig. 2-1); 2) four-part dental bridges from 1-st premolar to 2-nd molar of the lower jaw (Fig. 2-2); 3) flat specimens for testing of tensile strength and adhesion strength of the coatings to dental alloys (Fig. 2-3).



*Fig. 2-1 Cubic samples of different polymers, 3D printed by DLP stereolithography.*

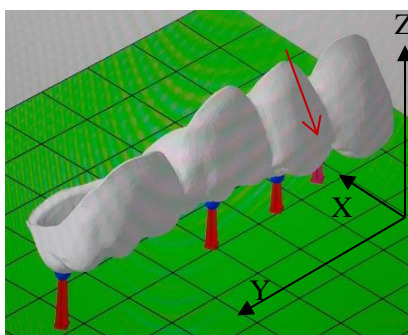


*Fig. 2-2 Virtual 3D model of four-part dental bridge.*

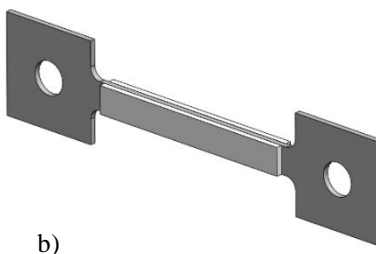
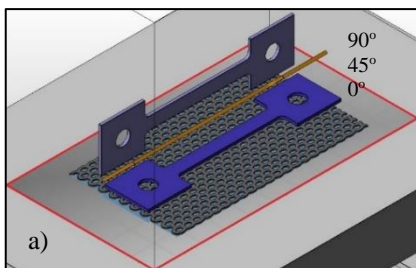


*Fig. 2-3 Scheme of ready for 3D print models for casting of samples of dental alloys (a) and sample with porcelain coating (b).*

## 2.1.2. Materials, technologies and equipment for samples manufacturing

### 2.1.2.1. Polymeric samples

The polymeric samples were produced using four types of AT processes – DLP stereolithography with printer *RapidShape D30* (*RapidShape*), laser assisted SLA – printer *Form 1+* (*Formlabs*), FDM with printer *Leapfrog Creatr Dual Extruder* (*Leapfrog*) and multi-jet printing - *SolidScape R66+* (*SolidScape*).

Materials, intended for application in dentistry and specific to each equipment type, were used. The printers *Rapid Shape D30* and *Form 1+* work with methacrylate photopolymers (Table 2-2) in liquid form, *Leapfrog Creatr Dual Extruder* – with polymer *PLA* (*Polylactic Acid*) in wire shape with diameter 1.75 mm, while *SolidScape R66+* with wax-like polymer.

Table 2-2  
PMMA polymer type and technological parameters in 3D printing by *Rapid Shape D30* printer.

Material	NextDent Base	NextDent Model	NextDent Model Ortho	NextDent C+B	NextDent Cast	NextDent Tray	NextDent Surgical Guide
Sample's position	1) Horizontal 2) Inclined at 45°						
Layer thickness [mm]	0,035	0,035	0,050	0,050	0,050	0,050	0,100
Color	Pink	Opaque beige	Opaque beige	A3,5 on Vita	Violet	Blue and pink	Transparent orange
Energy, mJ/dm <sup>2</sup>		550	430	460	460	410	650

Table 2-3  
Chemical composition of the alloys used in investigation.

Alloy	Chemical composition, wt. %									
	Co	Cr	Mo	Si	Mn	C	Fe	Ni	B	Nb
<i>Co-Cr alloys</i>										
<b>ASTM F75</b>	Bal.	27-30	5-7	<1	<1	<0,35	<0,75	<0,5	-	-
Biosil-F (Degudent) for catins	64,8	28,5	5,3	0,5	0,5	0,4	-	-	-	-
i-Alloy (i-Dental) for casting	64	30	5	-	-	0,5	-	-	-	-
Co212-f ASTM F75, for SLM	65,2	28,3	5,48	0,754	-	-	0,164	-	-	-
<i>Ni-Cr alloys</i>										
Wiron light (Bego) for casting	-	22.0	10.0	2.1	< 1	-	-	64.6	<1	<1

### 2.1.2.2. Samples of dental alloys

Four alloys of two systems - Co-Cr and Ni-Cr (Table 2-3) were used for investigation the properties of dental alloys produced using AT. *Co212-f* alloy is especially designed for the SLM equipment. In order to make a comparative analysis of the properties of dental alloys fabricated by casting and SLM, a *Biosil-F* alloy, having a chemical composition closest to that of *Co212-f*, was selected.

- *Cast samples*

Two different types of specimens were produced - four-part dental bridges and flat samples for tensile tests. The cast patterns for them were manufactured conventionally by wax or by 3D printing of the relevant polymer.

The samples were cast of Co-Cr alloys *Biosil-F* (*Degudent*) and *i-Alloy* (*i-Dental*) as well as Ni-Cr alloy *Wiron light* (*Bego*) using machine for induction melting and casting *Castomat Krupp table*.

- *SLM samples*

Two groups of samples were manufactured of *Co212-f* ASTM F75 alloy using machine *SLM 125* (*SLM Solutions*), equipped with Nd:YAG laser (Fig. 2-7). The first group were four-part dental

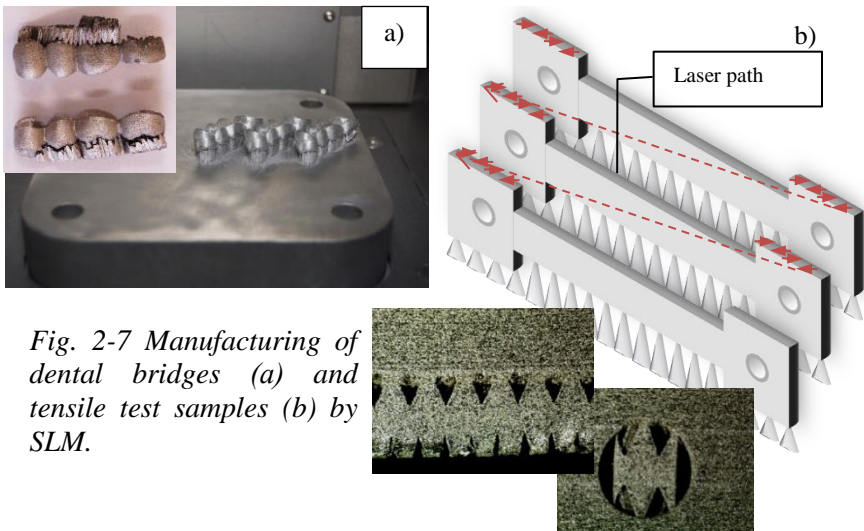


Fig. 2-7 Manufacturing of dental bridges (a) and tensile test samples (b) by SLM.

bridges, the second – flat tensile test specimens. The details were fabricated with regimes, recommended by the company producer of the equipment.

- *Samples for investigation the adhesion strength of porcelain and composite coatings to dental alloy*

For study the adhesion strength of porcelain and composite coatings to dental alloys, tensile test specimens were produced using three different technologies - conventional casting, casting with 3D printed patterns and SLM. Before porcelain firing, the surfaces of the cast samples were sandblasted for 8 s with alumina (*Cobra Aluoxyd weiß*, 250  $\mu\text{m}$ ) under 6 atm pressure and than were steam-jet cleaned. In contrast, in order to preserve the original roughness, the SLM samples were not sandblasted, but only cleaned in a steam-jet machine.

Depending on the type of research, a 1.1 +/- 0.1 mm thick layer of porcelain *IPS InLine (Ivoclar Vivadent)* or *Crea.align set 12* composite was applied and fired on both sides, following the manufacturer's instructions.

## 2.2. ACCURACY AND ROUGHNESS INVESTIGATIONS

### 2.2.1. Geometrical accuracy

The geometrical accuracy of the additively manufactured dental materials was examined using cubic samples and four-part bridge constructions. The dimensions of the sides ( $a$ ,  $b$ ,  $c$ ) and the diagonals ( $d1$ ,  $d2$ ) of the cubic samples were measured, while in the dental bridges - the dimensions of the connectors between the bridge bodies and the bridge retainers ( $a1$ ,  $a2$  and  $a3$ ), the width of the bridge bodies

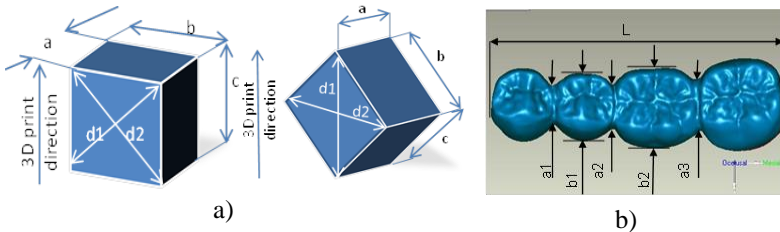


Fig. 2-8 Schemes of the dimensions measurements of cubic samples (a) dental bridge (b).

( $b1$ ,  $b2$ ) and the length of all bridges -  $L$  (Fig. 2-8). The mean values of the dimensions, their maximum, minimum and average deviations were calculated.

### 2.2.2. Fitting accuracy of dental bridges

The fitting accuracy of the four-part bridge constructions to the gypsum model has been investigated in two ways - using a silicone test and a new, specially developed methodology based on engineering CAD software.

In the first case, a modified silicon test was used, in which the thickness of the silicon impression was measured at 6 points along the preparation boundary of the crowns (Fig. 2-9-a). The thickness of the impression determines the gap between the abutment teeth of the gypsum model and the crown-retainers of the bridge. This methodology does not guarantee high accuracy because: 1) the gap is calculated indirectly; 2) the silicon impression material is elastic and capable for deforming during the measurement.

In the present work, based on engineering CAD software, a new *in-vitro* methodology for study the gap between dental constructions and the prepared teeth has been developed. For this purpose, the bridges and gypsum pattern were scanned using *Tizian Smart-Scan* and *Exocad* software, and virtual models were generated. The virtual

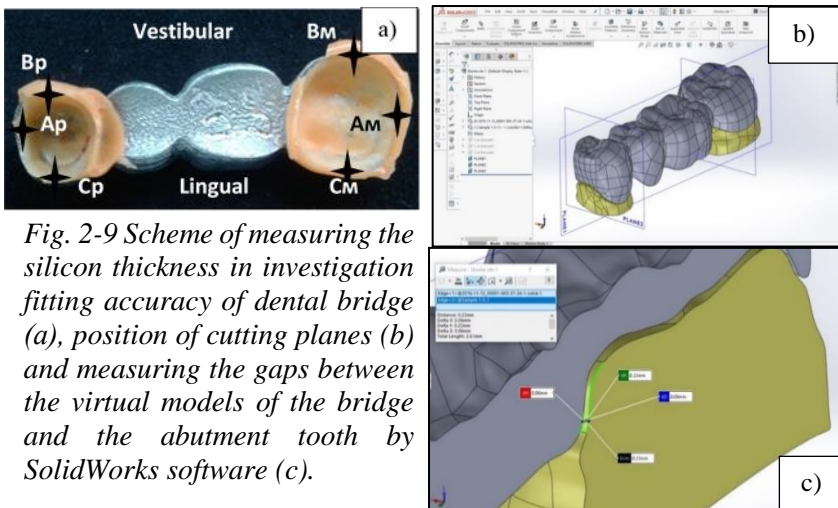


Fig. 2-9 Scheme of measuring the silicon thickness in investigation fitting accuracy of dental bridge (a), position of cutting planes (b) and measuring the gaps between the virtual models of the bridge and the abutment tooth by SolidWorks software (c).

models of the bridges were placed onto the virtual model of gypsum supports with the options provided by *SolidWorks* CAD software (Figure 2-9-b). The advantages of the newly developed methodology include: 1) it belongs to the group of non-destructive *in-vitro* methods; 2) it can be used to measure the fitting accuracy not only of dental bridges but also of a number of dental constructions such as inlays, onlays and crowns; 3) it allows to track the change in the distance between the surfaces of the dental constructions and the teeth in different directions; 4) distances on the three axes can be measured as well as the perpendicular between the surfaces and 5) it provides an order of magnitude higher accuracy (0.01 mm) than the silicone test.

### **2.2.3. Roughness investigation**

The roughness of additively manufactured materials was investigated by measuring the mean arithmetic deviation  $Ra$  with a *Taylor Hobson Surtronic 3* profile meter. The average values of  $Ra$ , maximum and standard deviations were calculated.  $Ra$  of the walls of the cubic samples, the vestibular surface of the second premolar of the four-part bridge constructions and the two working surfaces of the flat tensile test specimens was measured. The surface of the samples was examined with an optical microscope *Olympos SZ51* and a binocular metallographic microscope *XJL-17A*.

## **2.3. INVESTIGATION OF DENSITY, MICROSTRUCTURE AND CHEMICAL COMPOSITION**

### **2.3.1. Density investigation**

The study of the samples manufactured of Co-Cr alloys by casting and SLM was done in two ways: 1) the density of the bridge constructions was experimentally determined by the water displacement method and 2) the quantitative ratio of dense structure/pores was calculated by means of CAD software.

### **2.3.2. Microstructure and chemical composition**

The microstructure and chemical composition of Co-Cr dental alloys have been investigated using metallographic samples, etched chemically and electrochemically. The *Olympos SZ51* optical

microscope, the *XJL-17A* binocular metallographic microscope and the "*SEM / FIB LYRA I XMU, TESCAN*" Scanning Electron Microscope (SEM) equipped with an EDX detector (*Quantax 200, Bruker*) were used.

#### **2.4. HARDNESS INVESTIGATION**

The hardness of Co-Cr dental alloys was measured by the micro-Vickers and Rockwell methods and an analysis was done using the Weibull model.

#### **2.5. INVESTIGATION TENSILE STRENGTH AND ADHESION STRENGTH OF COATINGS ON DENTAL ALLOYS**

A combined study of tensile strength and adhesion strength of porcelain and composite coatings to dental alloys was carried out by experiments, regression analysis and numerical modeling with the Finite Element Analysis (FEA).

##### **2.5.1. Experimental investigation**

Measurement of tensile strength, determination of yield strength and modulus of elasticity of dental alloys were performed on a standard testing machine *FM-1000*. Flat samples were used for tensile tests, while for experimental investigation of adhesion strength of ceramics and composite to dental alloys - two-sided covered tensile test blanks. The modulus of elasticity was calculated according to the method in [Dolgov N.A. (2004)], and the shear stresses  $\tau$ , characterizing the adhesion strength of the coatings, were determined by the formulas given in [Umanskij E.C. and Lyshenko B.A. (1975)]:

$$\tau = \frac{k\varepsilon}{1/(E_s H) + 1/(E_c h)} \tanh(kl), \quad (3)$$

Where:

$$k = \sqrt{L \cdot \left( \frac{1}{E_s H} + \frac{1}{E_c h} \right)}; \quad (4)$$

$$L = 2 \left( \frac{G_s}{H} \cdot \frac{G_c}{h} \right) \bigg/ \left( \frac{G_s}{H} + \frac{G_c}{h} \right); \quad (5)$$

Where:

$E_s, E_c$  – elastic modulus of the substrate and the coating respectively;  
 $G_s, G_c$  – shear modulus of the substrate and the coating respectively;  
 $2H, h$  – thickness of the substrate and the coating respectively;  $\varepsilon$  – substrate strain at which occurs delamination of the coating;  $l$  – crack spacing in a fragmented coating.

For the first time, adhesion strength of ceramic and composite coatings was investigated by tensile test of dental alloys. The advantage of the proposed approach compared to ISO Standard 9693-1: 2012 is the ability to determine the adhesion strength of a coating not only of porcelain but also of composite.

The failure mode of the porcelain coating was evaluated by visual inspection and microscope observation. The surface of the specimens was examined before and after the tests using an optical microscope *Olympus SZ51*, a binocular metallographic microscope *XJL-17A* and a scanning electron microscope *Jeol 733 Microprobe*.

Until now, there is no unified criterion for determining the fracture type of porcelain coating from the metal base. For a more precise determination of the failure mode of the porcelain coating from dental alloys, an improved criterion is proposed and used in the present work. It was developed based on the methods of Han X. et al. (2018) and Dimitriadis K. et al. (2018), where the type of rupture is estimated by the amount of porcelain remaining on the surface of the metal base. Definitions of adhesive and cohesive mode of disruption are the same as proposed by Han X et al. (2018) - with up to 20% and over 80% ceramic on the surface of the metal base, respectively. Unlike [Han X. et al. (2018)] we suggest that the mixed type of rupture (with 20% - 80% residual porcelain on the surface) to be divided into two sub-ranges: in 20%-50% ceramic residues to define a mixed/adhesive mechanism, while in 50%-80% - mixed/cohesive.

### 2.5.2. Regression analysis

A regression analysis of the results of the measurements of the mean arithmetic deviation of the roughness  $Ra$  of the Ni-Cr alloy and the adhesion characteristics of the ceramic coating was performed using the *Mathcad* and *MADMML* software products.

### 2.5.3. Numerical modeling

Numerical modeling was done by FEA using *Solid Works* software. The tensile strength and adhesion strength of porcelain to dental alloys, manufactured by conventional casting, casting with 3D printed patterns and SLM, were studied. For this purpose, virtual models have been created with the shape and dimensions of the real samples (Fig. 2-11). The analysis was done using *Solid Works Simulation* software. In the present study, three Co-Cr dental alloys: *Biosil-F* (conventionally cast), *Co212-f* ASTM F75 (manufactured by SLM) and a *Wiron light* Ni-Cr alloy (cast with 3D printed patterns) were used. The chemical composition and the mechanical properties are given in Table 2-3 and Table 2-6. In the simulation process of the tensile test of specimens with no ceramic coating, a linear static analysis with a linear isotropic strengthening of the material was used. The stresses and the deformations in the maximal load of 10 000 N were obtained. The equivalent *von Mises* stresses and the Factor Of Safety (FOS) were evaluated.

In the adhesion strength simulations, a non-linear task was used. In its solution, data from the real tensile test were used for mechanical

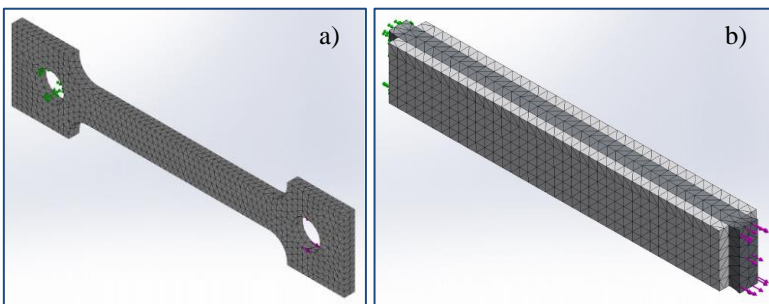


Fig. 2-11 Virtual models (fixing, external load and mesh), used in the simulation processes of tensile strength (a) and adhesion strength (b).

properties of the material. The loading force/deformation data, obtained in the tensile tests of all-metallic samples, were transformed into stress/relative strain curves which were used in the FEA.

Table 2-6.  
*Mechanical properties of dental alloys.*

Alloy	Yield strength R <sub>p0.02</sub>	Tensile strength R <sub>m</sub>	Modulus of elasticity E	Poisson Coefficient
	MPa		GPa	
Biosil-F	235*	400*	220 [61]	0.29 [300]
Co 212-f ASTM F75	520*	700*	220 [114]	0.29 [300]
* The yield strength and tensile strength values are calculated from the results of the tensile test.				

The stress investigation is done with the following assumptions for: 1) homogeneity of the materials, 2) linear elastic isotropic behavior of the porcelain and 3) nonlinear elastic behavior of Co-Cr alloys defined by experimental stress/relative strain curves. The normal and shear stresses as well as the equivalent stresses on the *von Mises* criterion, which act in the volume of the both materials of the sample - porcelain and Co-Cr alloys and at the boundaries between them, have been obtained and analyzed during the simulation. The change of the normal and equivalent stresses with the loading increase is evaluated.

## 2.6. BENDING STRENGTH INVESTIGATION

The bending strength of Co-Cr dental alloys has been investigated with a newly developed methodology, including experiment and simulation with CAD software of four-part bridge constructions produced by conventional casting, casting with 3D printed patterns and SLM.

The most loaded FPDs - dental bridges from 1-st premolar to 2-nd molar were used as samples. In order to be able to perform the load on the bridges as close as possible to the actual during bending process, the bending device was designed using CAD software according to a specially developed methodology. To fix the contact points between the bridge construction and the punches of the bending

device, a chewing load simulation was at first performed and on this basis, the device itself was designed.

### 2.6.1. Simulation of four-point bending test

The simulation of four-point bending test was done by FEA using *SolidWorks Simulation* software. Virtual models of the real bridges, manufactured by the mentioned above three technologies, were used in the investigation. The virtual models were created by the method, explained in point 2.2.2.

Two Co-Cr dental alloys were investigated – cast *Biosil-F* and SLM *Co212-f* ASTM F75 with chemical composition and mechanical properties given in Table 2-3 and Table 2-6. The values of the modulus of elasticity, yield strength and ultimate tensile strength, used in the FEA, were calculated in our experiments. The simulation analysis of the stresses was done with assumption for homogeneity of materials and linear elastic isotropic behavior.

The aim of the simulation was to create conditions closest to the real experiment. That is why the 3D virtual models of the four-part bridges were fixed at three points on the inner surfaces of the crowns-retainers, thus eliminating their rotation and translation. The loading was applied parallel to the vertical axis by means of two spherical elements only on the pontics (Fig. 2-14). Each element was contacted at three points on the occlusal surfaces of the second premolar and the first molar, similar to the punches used in the experiment. The task, performed by the simulations, was non-linear and the load changed from 0 to 20 000 N as that in the test. This allowed the results for different load values to be output.

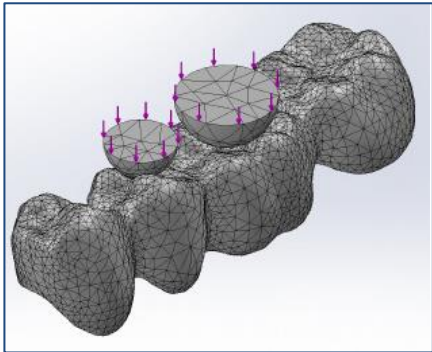


*Fig. 2-14 Scheme of the external load and mesh during simulation of four-point bending test.*

The deformations at maximum load were obtained and analyzed as well as the change of the normal stresses in the most loaded sections was monitored with the load increase. An evaluation of the equivalent stresses was performed on the *von Mises* criterion and the most probable sites of the samples failure were prevised.

### 2.6.2. Four-point bending test

Four-point bending test of Co-Cr dental bridges, manufactured by conventional casting, casting with 3D printed patterns and SLM was performed using especially designed test device. Universal tensile/compression test machine *Tira Test 2300 SE/50kN* (Fig. 2-15) was used during the experiment, which was realized with 1.2 mm/min loading rate until complete failure of the samples. Due to the complex shape of dental bridges, the loadings of crack initiation and complete failure were evaluated. Optical microscopy *Olympos SZ51* was used for observation of fracture surfaces.



*Fig. 2-15 Bending test of four-part dental bridges.*

## 2.7. TRIBO-CORROSION TEST

To investigate the tribological properties of Co-Cr dental alloys produced by casting and SLM, a *Nanovea Microtest SMT/A* tribometer of the type “ball-on-disk” was used, equipped with a tribo-corrosion apparatus. The samples of the two alloys (cast *Biosil-F* and SLM *Co212-f* ASTM F75) were mounted in epoxy resin. The test surfaces were grinded with SiC sandpaper and polished with diamond paste.

The molded alloys, having equal contact areas, were fixed into a polymeric chamber and polished surfaces were subjected to a

Fusayama-Meyer artificial saliva solution (KCl (0,4 g/l), NaCl (0,4 g/l), CaCl<sub>2</sub>.2H<sub>2</sub>O (0,906 g/l), NaH<sub>2</sub>PO<sub>4</sub>.2H<sub>2</sub>O (0,690 g/l) Na<sub>2</sub>S.9H<sub>2</sub>O (0,005) g/), Urea (1 g/l) with pH ~ 7.1. The counterpart material was selected as ZrO<sub>2</sub> having 3 mm diameter and the tests were carried out under 5N normal load, at a speed of 0.01 m/s during 100 m for 3 ½ h. All test results were evaluated by (i) variation of friction coefficient (COF) as a function of sliding distance, (ii) determination the change in weight, (iii) worn surface examinations by SEM.

## **RESULTS**

### **THIRD CHAPTER**

#### **ACCURACY AND ROUGHNESS OF DENTAL POLYMERS AND ALLOYS, MANUFACTURED BY ADDITIVE TECHNOLOGIES**

The accuracy and surface roughness of the dental constructions are of particular importance for their successful long-term work in the oral cavity. When talking about dental prostheses, the accuracy means not only the accuracy of their dimensions, but also the accuracy of their fitting to the prepared teeth. The roughness of the surfaces, on the one hand, affects these parameters of the construction itself and, on the other, the durability and corrosion resistance of the materials from which it is made. Its influence is further increased by the denture's working conditions - a significant variable mechanical impact in the aggressive environment of the saliva. Therefore, the accuracy and roughness of dental materials, manufactured using AT, should not be considered independently.

#### **3.1. ACCURACY AND ROUGHNESS OF DENTAL POLYMERS, FABRICATED BY STEREOLITHOGRAPHY**

The peculiarities of the technological processes of 3D printing, the properties of the polymers used and the position of the samples in

relation to the base or built direction affect the geometrical characteristics and the surfaces roughness of the dental constructions.

### 3.1.1. Dimensional accuracy

In the present study the geometrical accuracy of PMMA dental polymers, fabricated using 3D printer *Rapidshape D30* was investigated. Initially, cubic samples were used, which were printed in two positions - horizontally and inclined at 45° to the basis with layer thickness recommended by the company manufacturer of the printer (Fig. 2-1 and Table 2-2). It should be noted that all polymers have different color and optical properties.

It was found that specimens made from transparent or translucent polymers with a high layer thickness of 100 µm and 50 µm had a more precise sizes than the specimens printed from opaque plastics with a low layer thickness of 35 µm (Fig. 3-3). The dimensions of the sides (a, b, and c) located in the plane of the base XY are the smallest, followed by the sides in the YZ plane and the Z axis associated with the printing direction.

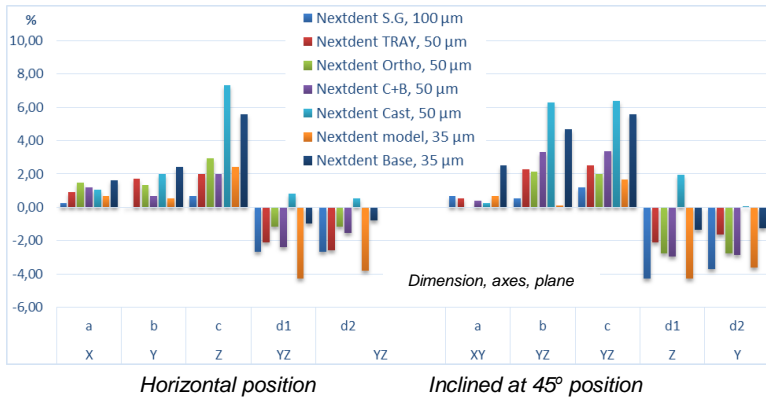


Fig. 3-3 Relative difference in % between dimensions of 3D printed cubic samples and the virtual model.

The present analysis showed that the different pigments in the particular dental polymers determine a different degree of reflection, absorption and transition of the light beam through the polymerization layer. Which, despite the different irradiating energy of each plastic,

results in significant differences in the dimensions. Therefore, the optical properties of dental polymers have a decisive influence on the accuracy of the constructions, manufactured by DLP stereolithography, compared to another two factors - the layer thickness and the position the object relative to the printing direction.

For the further study, polymers were selected to produce identical constructions but of different color: *NextDent C + B* for fabrication of temporary crowns and bridges with color close to natural teeth and *NextDent Cast* - with a darker violet color, designed for printing of patterns for casting of FPDs or frameworks for them from dental alloys. Using the *Rapidshape D30* printer, two types of specimens - cubic, positioned horizontally and inclined at 45° towards the base, and 4-part dental bridges were printed with a different layer thickness (recommended by the manufacturing company 50 μm and lower - 35 μm) (Fig. 2-2).

The study had shown that samples of the two polymers, manufactured in a horizontal position with a lower layer thickness of 35 μm, had a higher dimensional accuracy. The most accurate are the dimensions parallel to the base - X and Y axes (-2.88% to 2.00% difference with the virtual model), and with the largest differences - those parallel or inclined to the printing direction Z axis (Fig. 3-6). Additionally, 3D printed samples of *NextDent Cast* polymer are more inaccurate, even though they are fabricated with the same technological parameters.

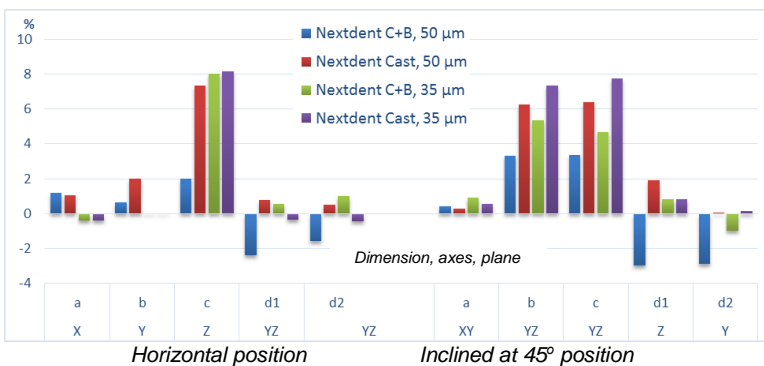


Fig.. 3-6 Relative difference in % between dimensions of 3D printed cubic samples and the virtual model.

The results of the present work have shown that in the studied range of the layer thicknesses, the dimensions of the cubic samples of the two polymers are influenced in addition to the optical properties and the position relative to the printing direction.

Examination of the accuracy of dental bridges, manufactured of *NextDent C + B* and *NextDent Cast* polymers, confirmed the results of the cubic sample experiment. In 3D printing of four-part bridges with a layer thickness of 35  $\mu\text{m}$ , the dimensions of the bridge bodies (b1 and b2) and the connectors between them (a1, a2 and a3) are smaller than those of the base bridge model with about 0.44% 2.20%

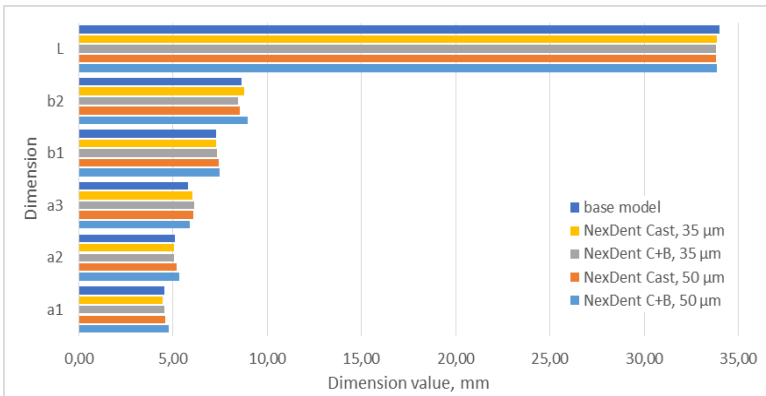


Fig. 3-7 Dimensions of polymeric dental bridges, 3D printed with different layer thickness.

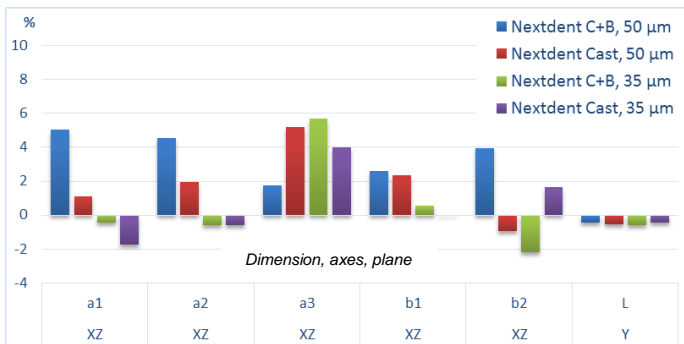


Fig. 3-8 Relative difference in % between dimensions of polymeric dental bridges, 3D printed with different layer thickness, with the dimensions of the bridge - base model.

(Fig. 3-7 and Fig. 3-8). While in fabricating with layer thickness of 50  $\mu\text{m}$ , recommended by the manufacturer, the dimensions are higher by 1.10% -5.17%. These dimensions are located at a slope of almost  $45^\circ$  in plane XZ (Fig. 2-2), as Z being the built direction. Their magnitude is commensurable and their position - analogous to the sides of the inclined cubic samples in the previous experiment.

In both polymers, there is a tendency for reduction of the dimensions and their maximum deviations with decreasing the layer thickness, i.e. the accuracy is increased. This confirms the assumption we have made about the decisive influence of the optical properties of polymers for obtaining a precise construction in the stereolithography process.

The investigation of details of dental polymers manufactured by DLP stereolithography showed that the optical properties of dental polymers have a decisive impact on the accuracy. The layer thickness and the energy density, required to obtain high precision constructions, are determined from them.

The location of the object (the size respectively) relative to the printer base or print direction is the next basic parameter that affects the accuracy. Regardless of the layer thickness, the most accurate are the dimensions located in the XY plane, parallel to the base. The dimensions, positioned in planes XZ, YZ or Z axis, related to the built direction, are characterized with the lowest accuracy. Decreasing the thickness of the layer in the stereolithography process leads to reducing the sizes of the object and to increasing the accuracy.

### **3.1.2. Fitting accuracy of dental bridges**

The investigation of the fitting accuracy of temporary bridges and cast patterns, 3D printed with the recommended layer thickness, have shown that the gap between the abutment teeth and the crowns-retainers is within the permissible limit but is unevenly distributed (Fig. 3-11). Decreasing the thickness of the building layer in some cases may result in zero values of the gap. These results confirm once again the thesis that the optical properties of the monomers used play a decisive role in the accuracy of the fixed partial dentures, manufactured by SLA.

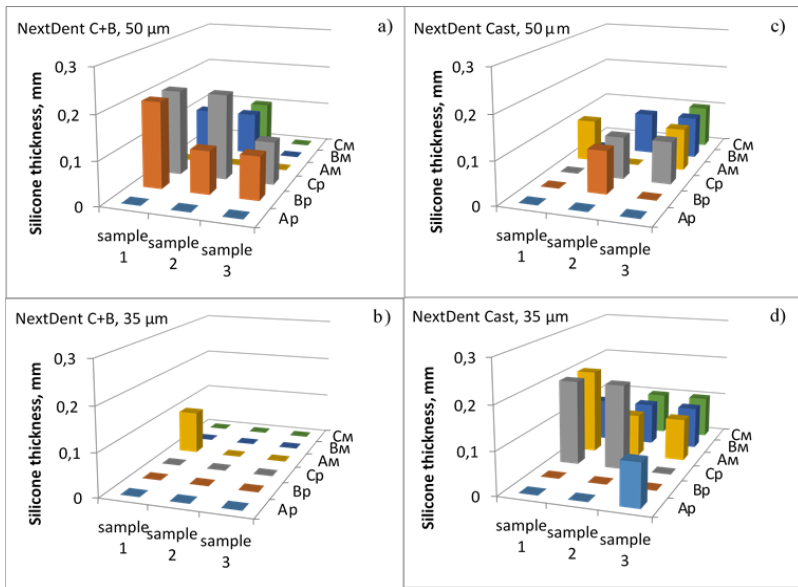


Fig. 3-11 Thickness of silicone probe in investigation of fitting accuracy of polymeric dental bridges.

### 3.1.3. Surface roughness

The data of roughness investigation show that the cubic samples positioned horizontally have a much smaller surface roughness than those printed on a slope (Fig. 3-12). The walls, located horizontally to the base, have the smallest roughness, while the roughness of the

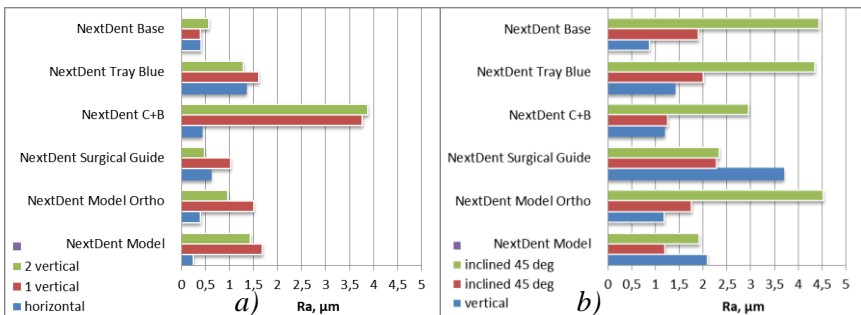


Fig. 3-12 Mean arithmetic deviation  $R_a$  of the surface roughness of 3D printed cubes of different polymers in horizontal position (a) and inclined at 45° to the base (b).

vertical walls is almost 3 times higher (Fig. 3-12-a). The vertical walls of plastic specimens with the thinner polymerization layer of 35-50  $\mu\text{m}$  are characterized by the smallest roughness. In the inclined specimens, the walls, positioned at 45° relative to the base, are characterized with the highest roughness (Fig. 3-12-b). The  $R_a$  values are smaller for the walls that are closer to the supports, i.e. those printed at the beginning of the process, and the largest for those printed at its end (Fig. 3-13).

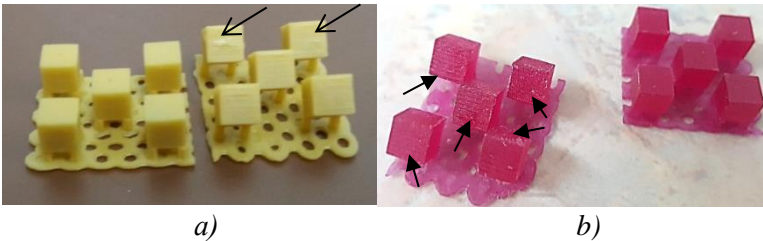


Fig. 3-13 Samples of polymers NextDent Model (35  $\mu\text{m}$ ) (a) and NextDent Cast (50  $\mu\text{m}$ ) (b).

In examining the influence of the layer thickness on the surface roughness in 3D printing of two groups of samples - cubic and 4-part bridge constructions, it was found that the roughness increases with increasing the layer thickness (Fig. 3-15 and Fig. 3-17). This tendency is characteristic for both the vertical and the inclined walls. Regardless of the layer thickness, the roughness of the *NextDent Cast* samples is 30-50% higher than that of *NextDent C + B*. Observation of the bridge surfaces with a light microscope confirms the above data (Fig. 3-18).

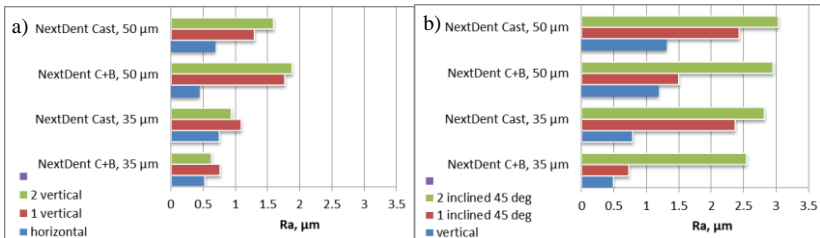
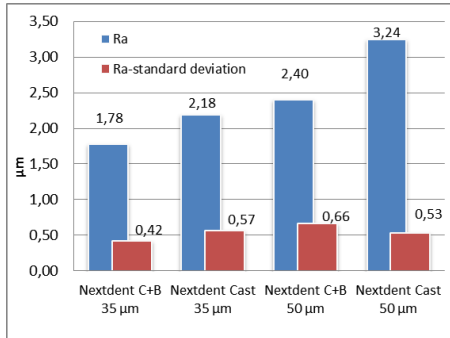
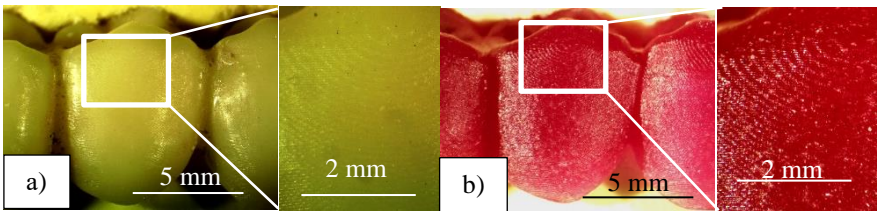


Fig. 3-15 Mean arithmetic deviation  $R_a$  of the surface roughness of cubic samples, 3D printed in horizontal position (a) and inclined at 45° to the base (b).

The traces of the individual layers, typical for the manufacturing by stereolithography process, can be clearly seen on the pictures.



*Fig. 3-17 Mean arithmetic deviation Ra of the surface roughness.*



*Fig. 3-18 Surface morphology of temporary bridges (a) and polymeric cast patterns (b), 3D printed with 50 µm layer thickness.*

An interesting feature is observed - inclined surfaces, that are formed at the end of the process by reducing the projection area, have a greater roughness than surfaces, that are inclined at the same angle but are obtained by increasing of the projections area at the beginning of the process, which may be associated with the optical properties of the monomers used.

In the present work it is confirmed that the thickness of the building layer and the position of the workpiece relative to the printing direction exert an influence on the roughness of the 3D printed dental plastics. It has been found that two more factors affect the surface roughness of dental polymers produced by DLP SLA - the optical properties of the monomers used and the formation of the surfaces at the beginning or the end of the process. The surfaces, parallel to the base, are characterized with the lowest roughness ( $Ra=0.5-0.7 \mu\text{m}$  for

nearly the all investigated polymers). Only the optical properties influence on their quality. The roughness of the surfaces, parallel or inclined at 45° towards the Z-axes, is 2-3 times ( $R_a=0.75-2.1 \mu\text{m}$ ) and 5-6 times ( $R_a=1.25-4 \mu\text{m}$ ) higher compared to the surfaces, parallel to the base. The highest roughness is characteristic for the surfaces of details, 3D printed of darker material at the end of the process with larger layer thickness and positioned inclined towards the built direction.

### 3.2. ACCURACY AND ROUGHNESS OF POLYMERIC BRIDGE CONSTRUCTIONS, PRODUCED BY STEREO LITHOGRAPHY AND FUSED DEPOSITION MODELING

The accuracy and surface roughness of polymeric dental bridges, produced of *PMMA* and *Poly-lactic Acid (PLA)* with 50  $\mu\text{m}$  layer thickness using 3D printers working on different principles – FDM, laser assisted and DLP stereolithography were investigated.

#### 3.2.1. Dimensional accuracy

Study of the geometrical characteristics of dental bridges have shown that the dimensions, parallel (Z-axes) or inclined (XZ plane) to

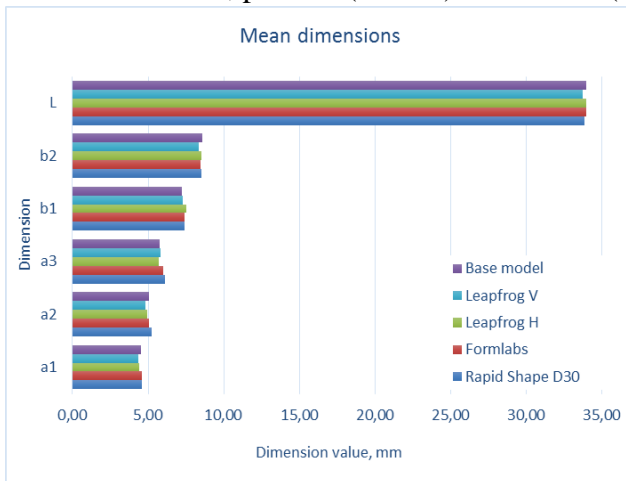


Fig. 3-19 Dimensions of polymeric dental bridges, manufactured by different 3D printers.

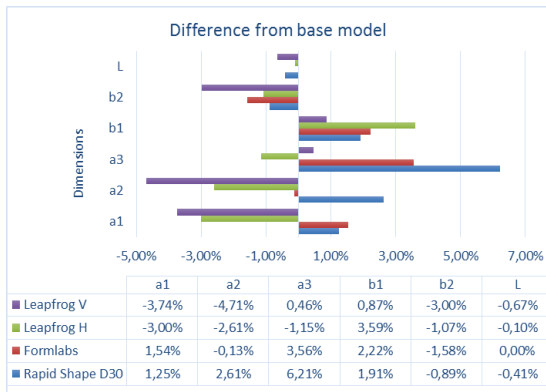


Fig. 3-20 Relative difference in % of the dimensions of dental bridges, manufactured by different 3D printers, with the dimensions of the base bridge – model.

the built direction, are characterized with the largest deviation (Fig. 3-19 and Fig. 3-20). In SLA samples, these dimensions are larger than the base bridge – model, while in the FDM samples they are smaller. The length of the dental bridges L, positioned along the Y direction and not related to the build direction, is comparatively accurate.

From the three printers types, the highest dimensional accuracy of the bridge constructions is ensured by printer *Form 1+* (*Formlabs*), working on the principle of laser assisted SLA.

### 3.2.2. Surface roughness

From the three technologies used, the DLP stereolithography process ensures the lowest surface roughness (Fig. 3-22), followed by the laser assisted SLA. The polymeric constructions, manufactured by FDM, are

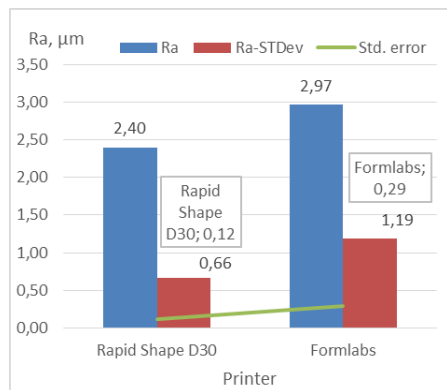
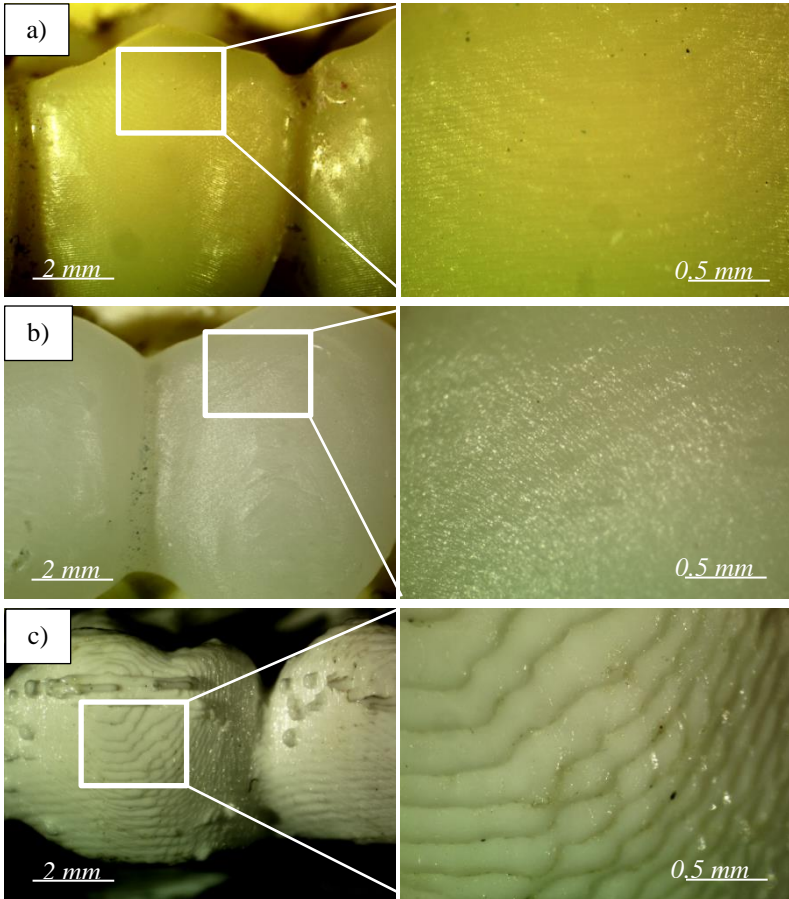


Fig. 3-22 Mean arithmetic deviation Ra of the surface roughness of polymeric dental bridges, produced by DLP and laser SLA. (*Rapid Shape D30* and *Formlabs* printers respectively).

characterized with the highest surface roughness. Regardless the types of the technological process, the individual building layers are clearly visible on the samples' surface (Fig. 3-23).

The present research showed that 3D printers, based on laser assisted and DLP SLA, can be successfully used for manufacturing of polymeric dental bridges. The deviations in the sizes of the constructions, produced by 3D printing, can be compensated during the process of building a virtual model, while the surface quality can



*Fig. 3-23 Surface morphology of polymeric dental bridges, produced by different 3D printing processes: DLP SLA (a), laser SLA (b) and FDM (c).*

be improved by additional mechanical or chemical treatments. Due to the high roughness of the details produced the FDM-based printer is suitable only for fabricating of training models.

### 3.3. ACCURACY AND ROUGHNESS OF Co-Cr DENTAL ALLOYS CAST WITH 3D PRINTED PATTERNS

The accuracy and surface roughness of Co-Cr dental alloys, cast with 3D printed patterns, were investigated using three groups of samples – four-part dental bridges. The specimens of the first group were cast of *Biosil-F* alloy as the cast patterns were manufactured by multi-jet 3D printer *Solidscape 66+* with layer thickness of 13  $\mu\text{m}$ . The bridge constructions of the second and third groups were cast of *i-Alloy* using cast patterns, 3D printed by the DLP stereolithographic equipment *Rapidshape D30*. The cast patterns for the second group of samples were printed with 35  $\mu\text{m}$  layer thickness, while these for the third group – with 50  $\mu\text{m}$ .

#### 3.3.1. Dimensional accuracy

The present study of Co-Cr dental alloys, cast with 3D printed patterns, has shown that the bridges, cast with patterns built with the lowest layer thickness of 13  $\mu\text{m}$  are characterized with the highest accuracy (-2.86%/+1.72% relative difference with the dimensions of

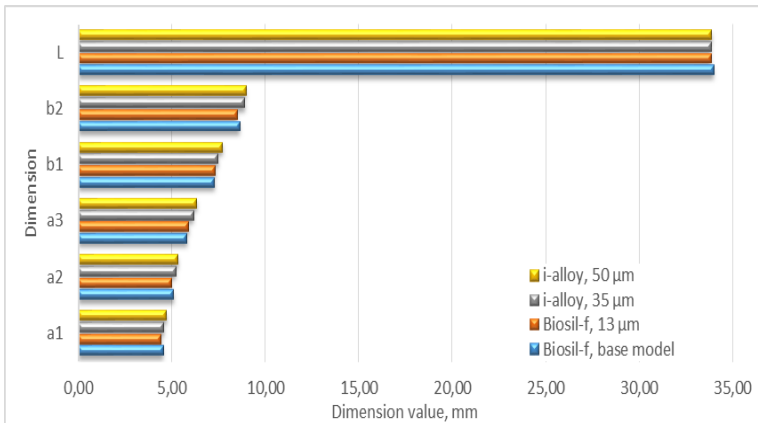
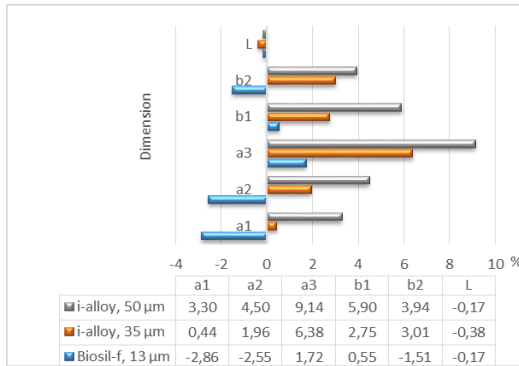


Fig. 3-25 Dimensions of cast bridges, manufactured using 3D printed cast patterns with different layer thickness.



*Fig. 3-26 Relative difference in % of the dimensions of dental bridges with that of the base model.*

the base bridge-model) (Fig. 3-25 and Fig. 3-26). Increasing the layer thickness in 3D printing of patterns leads to increasing the dimensions of the Co-Cr dental bridges. The dimensions of the bridge constructions, cast from 3D printed patterns with 50 μm layer thickness (recommended by the company producer), characterize with the largest values (3.30%-9.14% larger than those of the base model).

In order to obtain precise construction of Co-Cr alloy in casting with 3D printed patterns, it is necessary to choose the appropriate layer thickness for manufacturing the cast pattern, ensuring accurate dimensions of the casting. If the recommended by the company layer thickness is used, the sizes of the constructions should be corrected with the proper coefficients still on the stage of the virtual model generating.

### **3.3.2. Fitting accuracy of Co-Cr dental bridges**

The gap between the crowns-retainers of Co-Cr bridge constructions and the abutment teeth of the gypsum model is 0-0.2 mm unevenly distributed (Fig. 3-28). It is in the acceptable range according to the clinical requirements. In order to ensure evenly distributed gaps of Co-Cr dental bridges, cast with 3D printed patterns, the measures for decreasing the deformations should be taken in both the casting of the constructions and manufacturing of the cast patterns.

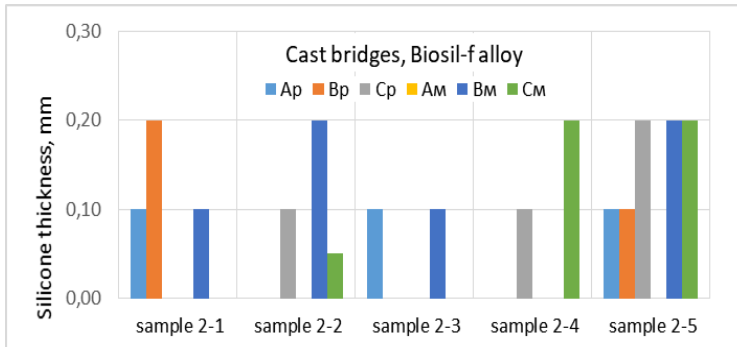


Fig. 3-28 Thickness of the silicone layer during measuring the fitting accuracy of dental bridges, cast of Biosil-f alloy with 3D printed patterns.

### 3.3.3. Surface roughness of Co-Cr dental bridges

The roughness of Co-Cr bridges, cast from the 3D printed patterns, is 3-4 times higher compared to the bridge-base model (Fig. 3-29), which is cast from conventional wax pattern. Increasing the layer's thickness of the 3D printed patterns leads to increase the roughness of the Co-Cr bridges ( $R_a=3.39 \mu\text{m}$  in pattern, 3D printed with  $13 \mu\text{m}$  layer thickness;  $R_a=3.69 \mu\text{m}$  and  $R_a=4.03 \mu\text{m}$  in patterns, built with layer thicknesses of  $35 \mu\text{m}$  and  $50 \mu\text{m}$  respectively). The typical layered morphology of the polymeric patterns remain on the

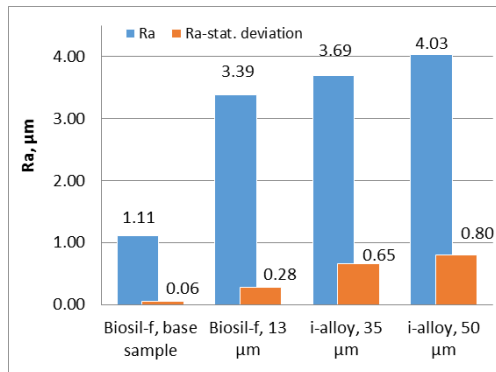


Fig. 3-29 Average arithmetic deviation  $R_a$  of the surface roughness of dental bridges, cast with 3D printed patterns.

metal surface after casting, cleaning and sandblasting, independently of the layer thickness of 3D printing process (Fig. 3-31).

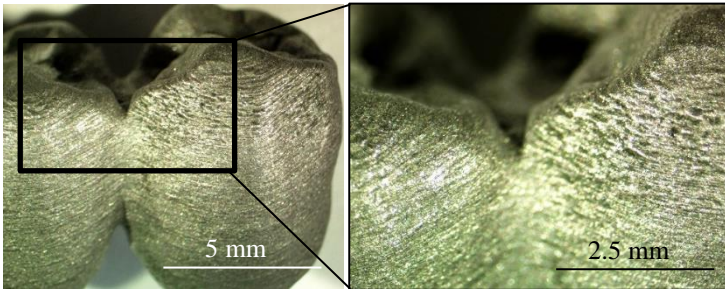


Fig. 3-31 Surface morphology of Co-Cr bridges, cast on patterns, 3D printed with 13  $\mu\text{m}$  layer thickness.

In production of all-metal constructions, the higher roughness is disadvantage and the metal surfaces should be polished. But in metalceramic and restorations, covered with composites and polymers, it could be expected the higher roughness to be an advantage, leading to increase of the adhesion strength between the porcelain/polymer/composite and the alloy.

### 3.4. ACCURACY AND ROUGHNESS OF Co-Cr DENTAL ALLOYS, PRODUCED BY SLM

The accuracy of Co-Cr dental alloys, produced by SLM, has been investigated using four-part bridge constructions. The samples are made of alloys with a close chemical composition (Table 2-3, Chapter 2): *Co212-f* ASTM F75 for SLM bridges and *Biosil-F* (*Degudent*) for the cast.

#### 3.4.1. Dimensional accuracy

In the study of the Co-Cr bridge constructions produced by SLM, it has been found that this technology guarantees the highest accuracy and repeatability of the dimensions (Fig. 3-32). The average dimensions of almost all elements of the bridges produced by the SLM are smaller than those of the base bridge-model with 0.07 mm - 0.23 mm.

### 3.4.2. Fitting accuracy of Co-Cr bridge constructions

The investigation of fitting accuracy of the bridge constructions to the abutment teeth was done by a silicone test and a newly developed methodology using *SolidWorks* CAD software. The results of the two methodologies show that the fitting accuracy of the SLM

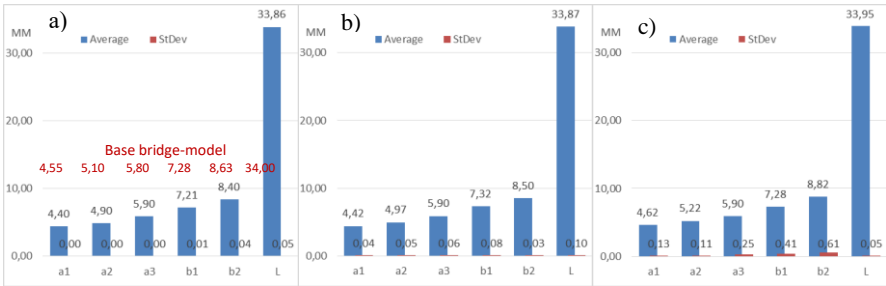


Fig. 3-32 Average values and standard deviations (StDev) of dimensions of dental bridges, manufactured by SLM (a), casting with 3D printed patterns (b) and conventional casting (c).

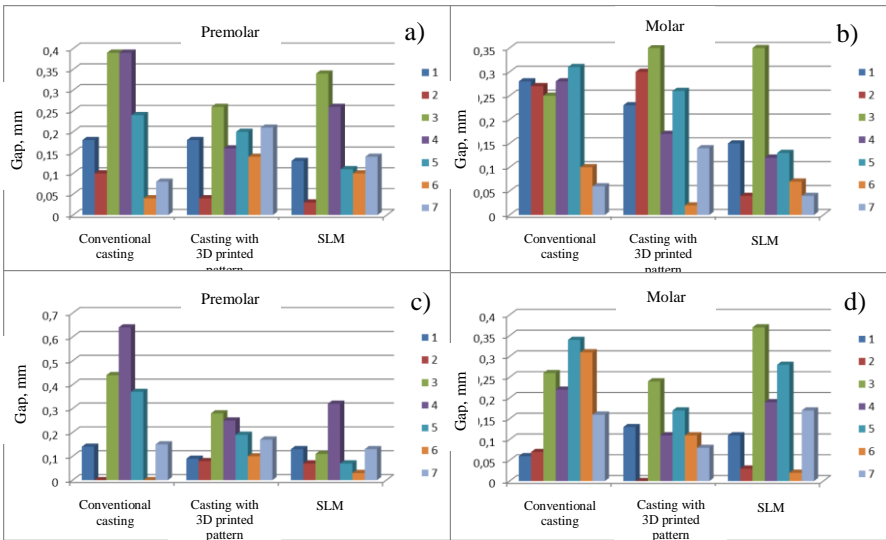


Fig. 3-34 Gap between the abutment teeth and crowns-retainers of virtual models of dental bridges in medial-distal (a) and (b) and vestibular-lingual (c) and (d) directions. (p. 1 and p. 7 – along the margins, p.2 and p.6 – between the vertical walls and p.3 – p.5 along the occlusal surface).

bridges is higher than that of the conventionally manufactured, but lower than the cast with 3D printed patterns (Fig. 3-34).

The gap along the marginal boundary and the inner gap of the bridges, made by SLM, are within a clinically acceptable range of 0.05-0.15 mm. The internal gap is unevenly distributed – it is the largest on the occlusal surfaces, followed by the marginal boundary and between the vertical walls.

### 3.4.3. Surface roughness of dental bridges

The roughness of Co-Cr dental alloys, produced by SLM, is about 4 times higher than conventionally fabricated and 30% greater than that of the alloys cast with 3D printed patterns ( $R_a = 4.24 \mu\text{m}$ ,  $R_a = 1.312 \mu\text{m}$  and  $R_a = 3.387 \mu\text{m}$ , respectively) (Fig. 3-35).

The higher roughness and peculiarities of the surface morphology of the SLM bridges are a limitation in its application for production of all-metallic constructions. However, when manufacturing restorations, covered with plastics/composite/porcelain, they

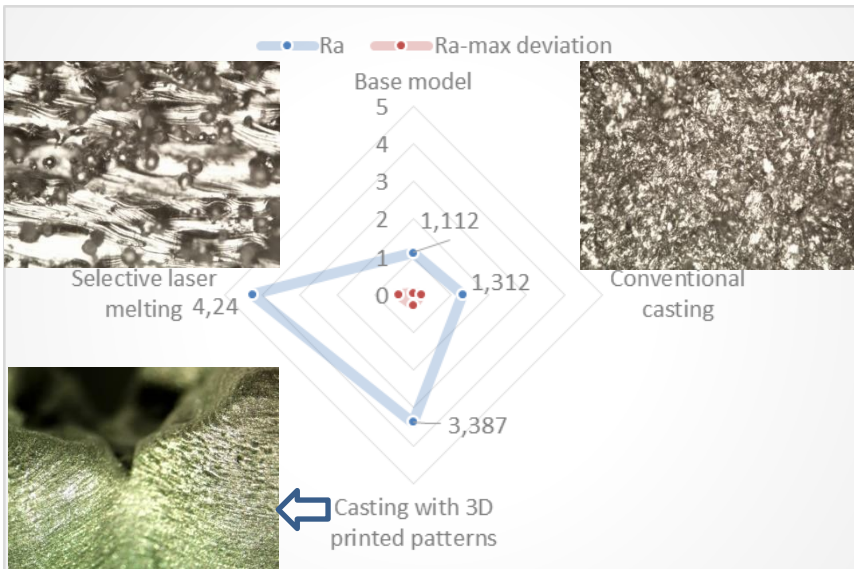


Fig. 3-35 Surface roughness and morphology of Co-Cr dental bridges, manufactured by different technologies.

can be advantageous and contribute to increasing the mechanical component of the coating's adhesion to the substrate.

## **FOURTH CHAPTER**

### **MICROSTRUCTURE AND HARDNESS OF DENTAL ALLOYS, MANUFACTURED BY ADDITIVE TECHNOLOGIES**

Traditionally the metallic frameworks of dental prostheses are manufactured by centrifugal casting on hand-made wax models, which is a prerequisite for low accuracy and satisfactory quality. Modern CAD-CAM systems provide the ability to produce customized high-quality constructions for short periods with high performance of the equipment. There are two main aspects for application of the additive technologies in production of metallic frameworks for dentures: 1) manufacturing of cast patterns by 3D printing and subsequent casting of the details, and 2) direct fabrication of the constructions from the 3D virtual model by selective laser melting.

#### **4.1. MICROSTRUCTURE OF DENTAL ALLOYS, MANUFACTURED BY ADDITIVE TECHNOLOGIES**

The special features of the manufacturing processes, technological regimes and production strategies, the type and parameters of

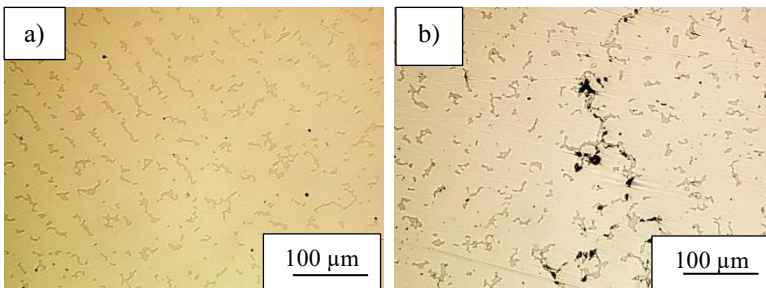


*Fig. 4-1 Microstructure of Co-Cr dental bridges, cast with 3D printed pattern (a) and conventionally manufactured wax pattern (b).*

the material used have a major impact on the microstructure of Co-Cr dental alloys.

#### 4.1.1. Microstructure of Co-Cr dental alloys, cast with 3D printed patterns

The microstructure of four-part bridges, cast from Co-Cr *Biosil-F* alloy with conventionally fabricated wax pattern and 3D printed pattern, was studied. It was confirmed that the microstructure of Co-Cr dental alloy, cast with additively manufactured models, is a typical cast structure - coarse grained and inhomogeneous with dendritic morphology (Fig. 4-1). It consists of  $\gamma$ -phase in the dendrites and small amounts of  $\epsilon$ -phase, while in the interdendritic spaces there are microeutectic and primary carbides of the type  $(Cr,Mo)_{23}C_6$  (Fig. 4-3). The microeutectic consists of  $\gamma$ -solid solution and intermetallic inclusions of the type  $Co_5(Cr,Mo)_3Si_2$ .

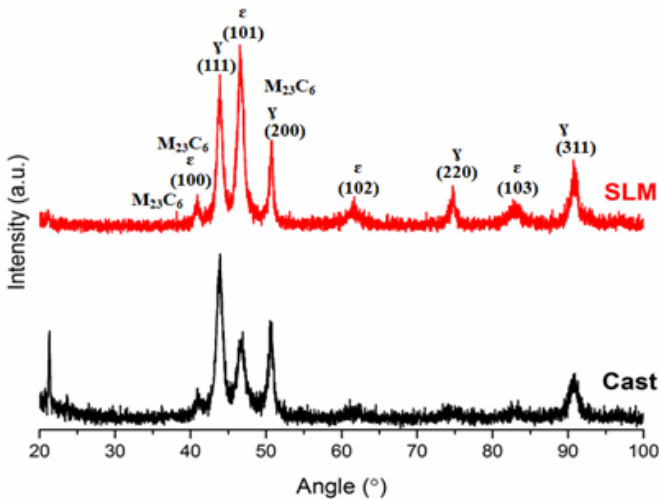


Fig. 4-3 XRD analysis of Co-Cr dental alloys, manufactured by casting (*Biosil-F*) and SLM (*Co 212-f*).

The specific coarse grained microstructure of cast Co-Cr dental alloys, characterized by dendritic morphology, inhomogeneous chemical composition and presence of  $\gamma$  and  $\epsilon$  phases in a different ratio, carbides and intermetallic compounds, determines their mechanical properties.

The defects of Co-Cr dental bridges, cast with 3D printed plastic patterns, are determined not only by the features of the casting process but also by the manufacturing technology of the cast pattern. These include, on the one hand, the typical for the castings inlets and gas pores and, on the other hand, 3 times higher surface roughness compared to conventional wax casting (Fig. 4-6 and Fig. 4-7). The found defects lead to lower density of the bridges cast from the Co-Cr *Biosil-F* alloy:  $7.86 \text{ g/cm}^3$  and  $8.03 \text{ g/cm}^3$  respectively for samples, cast conventionally and with 3D printed patterns, compared to the density, given by the manufacturer -  $8.4 \text{ g/cm}^3$ .

The defects of Co-Cr dental bridges, cast with conventional wax or 3D printed plastic patterns, are mainly determined by the features

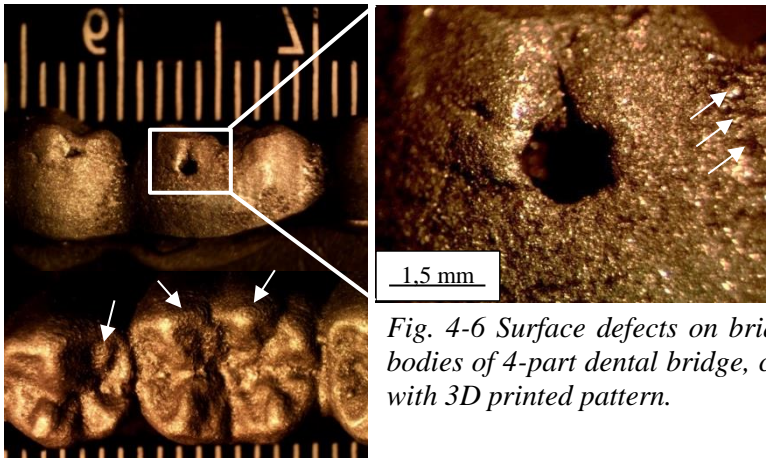


Fig. 4-6 Surface defects on bridge bodies of 4-part dental bridge, cast with 3D printed pattern.

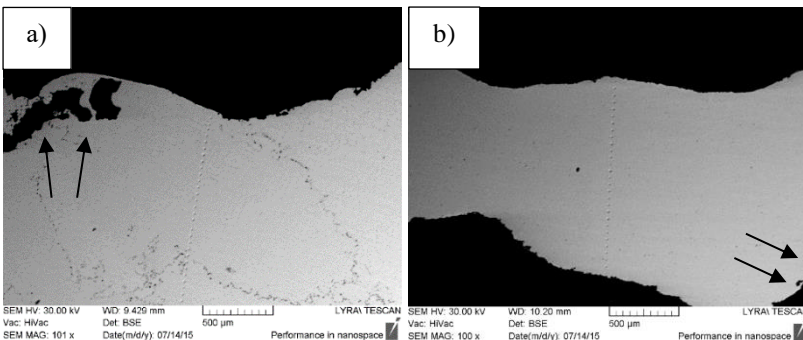
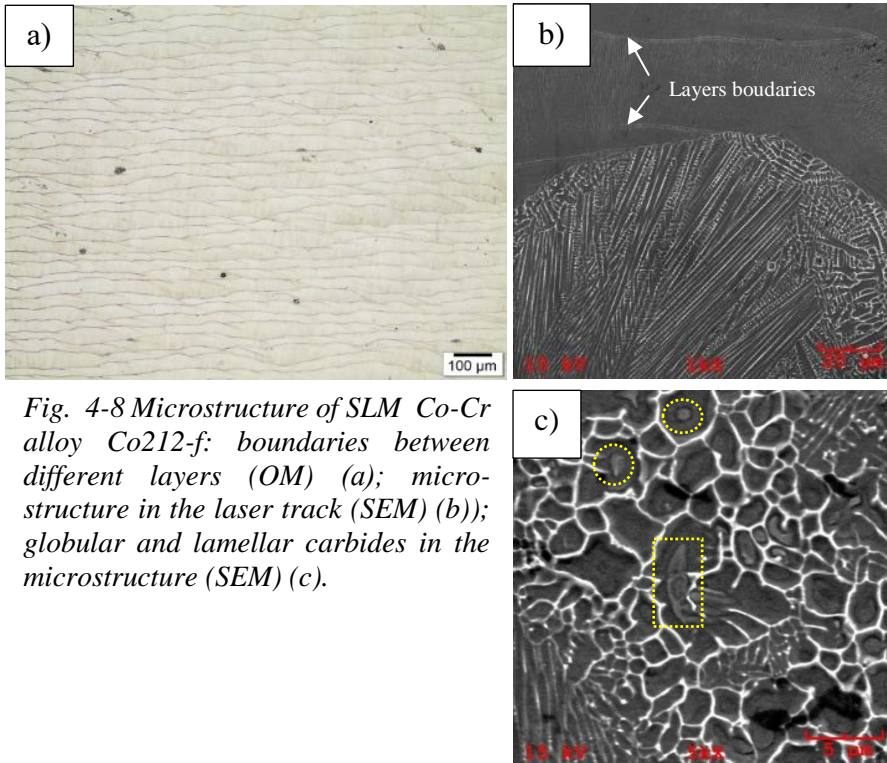


Fig.4-7 Microstructural defects of dental bridges cast conventionally (a) and with 3D printed pattern (b).

of the casting process. The manufacturing technology of the cast patterns influences the surface morphology of the details. In order to obtain non-defective constructions with high smoothness in casting with additively manufactured cast patterns, it is necessary to: 1) make a proper selection of the 3D printing process and apparatus; and 2) strict adherence to the technological regimes and operating rules during 3D printing and casting.

#### 4.1.2. Microstructure of Co-Cr dental alloys, produced by SLM

In the process of selective laser melting, the workpiece is obtained by successively melting layers of powdered material one on top of each other by means of a laser. During building of the construction, complex physico-chemical and metallurgical processes run in the area of laser impact - complete and partial melting of the



*Fig. 4-8 Microstructure of SLM Co-Cr alloy Co212-f: boundaries between different layers (OM) (a); microstructure in the laser track (SEM) (b); globular and lamellar carbides in the microstructure (SEM) (c).*

starting material, formation and growth of new phases and grains both in the molten pool and partially melted particles, solid state sintering, solid state phase transformations in the heat affected zone. All of these processes are realized at high heating and cooling rates and high temperature gradients. As a result, details are obtained with a specific fine-grained microstructure, which determines the characteristic higher mechanical properties.

The macrostructure of Co-Cr alloy *Co212-f*, produced by SLM, is characterized by clearly visible layers and boundaries between them (Fig. 4-8-a). The microstructure is fine and homogeneous in terms of chemical composition. It has dendritic morphology with  $\gamma$ -phase in the dendrites, presence of increased amount of  $\epsilon$ -phase and carbides of mixed type  $M_{23}C_6$  (Fig. 4-3). The results obtained confirm the research of other scientists in this field.

The most characteristic defects of the SLM components are the high surface roughness (4 times higher than conventionally cast alloy) and the porous structure (Fig. 4-10 and Fig. 4-11), as the ratio of dense structure/pores reaches 87.47% /12.53%.

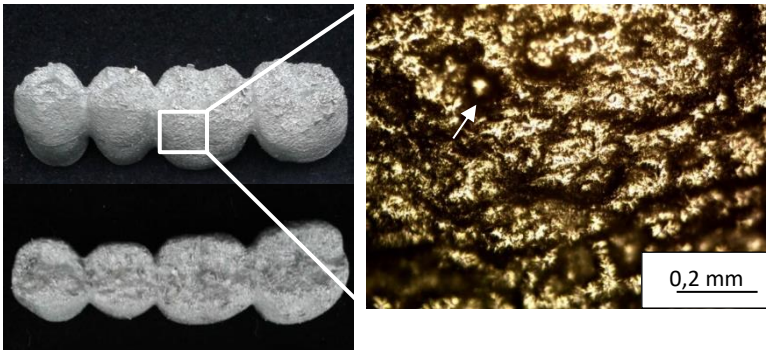


*Fig. 4-10 Surface defects on the bridge bodies of 4-part dental bridge, produced by SLM.*

In order to achieve high mechanical properties, it is important that the details, produced by SLM, are of high density and optimal surface quality. Minimization of defects can be achieved by optimization the parameters of the SLM process.

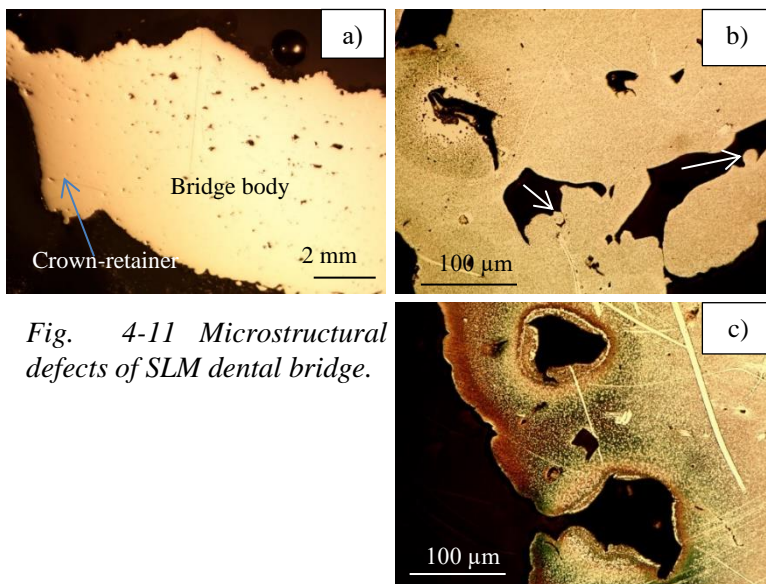


*Fig. 4-11 Microstructural defects of SLM dental bridge.*

The low energy density  $E$  is one of the main reasons for the observed porous structure. Since, according to formula (10), it is directly dependent on the laser power and in contrast to the scanning speed, these are the two most important technological parameters, by correcting which a dense structure can be achieved. The other reasons are the shape of the molten pool, the thickness of the building layer and the insufficient overlapping degree of the individual traces in the layer.

$$E = \frac{N}{vl_c t_c}, \quad (10)$$

Where:  $E$  is energy density [ $\text{J}/\text{mm}^2$ ],  $N$  is laser power [ $\text{W}$ ],  $V$  – scanning speed [ $\text{mm}/\text{s}$ ],  $l_c$  – distance between the particular molten tracks in one layer [ $\text{mm}$ ],  $t_c$  – thickness of the building layer in SLM process [ $\text{mm}$ ].

Therefore, the correct selection of the basic technological parameters - laser power, speed and scanning strategy that affect the shape and dimensions of the molten pool and hence the porosity and microstructure - will ensure the obtaining of details with dense microstructure and comparatively good surface quality.

## 4.2. HARDNESS OF Co-Cr DENTAL ALLOYS, MANUFACTURED USING ADDITIVE TECHNOLOGIES

The characteristic microstructure of Co-Cr dental alloys, produced by various technological processes - casting and selective laser melting, predetermines a difference in the hardness of the resulting constructions.

In the present work, a study of the hardness of Co-Cr dental alloys, manufactured using additive technologies, has been done. The hardness along the depth of all components of Co-Cr dental bridges, cast with 3D printed patterns and made by SLM, was measured (Fig. 4-13).

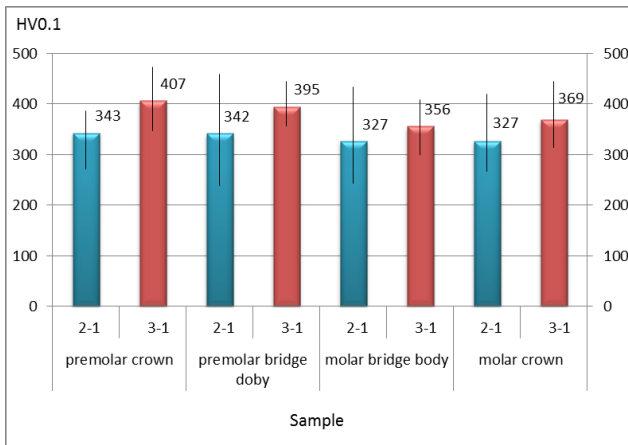


*Fig. 4-13 Average hardness of dental bridges, cast with 3D printed patterns of Biosil-F alloy (2-1) and produced by SLM of Co212-f alloy (3-1).*

### 4.2.1. Hardness of Co-Cr dental bridges, cast with 3D printed patterns

It has been found that the hardness of Co-Cr bridges cast with 3D printed patterns is in the range from 326 HV0.1 to 343 HV0.1 with uneven distribution and fluctuation of values within a broad range of +/-57 HV0.1 to +/-110 HV0.1, due to the specific coarse and inhomogeneous microstructure.

#### **4.2.2. Hardness of Co-Cr dental alloys, produced by SLM**

The hardness of the Co-Cr dental alloy *Co212-f*, produced by SLM (356 HV0.1-407 HV0.1), is about 13% higher than that of the *Biosil-F* alloy, cast with 3D printed patterns, and is characterized by a more even distribution in the sample's volume due to the characteristic fine-grained, relatively homogeneous microstructure and increased  $\epsilon$ -phase content.

The analysis, made by the Weibull model, showed that the shape parameter -  $c$  of the SLM alloy was larger than that of the cast alloy (32.3 and 10.3 respectively). This is an indication of a more homogeneous structure of the SLM alloy *Co212-f* compared to the cast *Biosil-F*, which is a precondition for its enhanced qualities.

The hardness of the two alloys - SLM *Co212-f* and cast *Biosil-F* changes in a different way after firing of two-sided porcelain coating on them. The hardness of the SLM specimens decreases to 36.5 HRC, while that of the cast increases to 39.8 HRC, which is determined by the different processes running in the microstructure during the thermal impact.

## **FIFTH CHAPTER**

### **STRENGTH PROPERTIES AND TRIBO-CORROSION OF DENTAL ALLOYS, MANUFACTURED BY ADDITIVE TECHNOLOGIES**

Dental alloys should have high mechanical properties to provide sufficient strength of the dental constructions, so that they can withstand the chewing efforts for a long time without deforming. In manufacturing of metalceramic fixed partial dentures their durability depends mainly on the adhesion strength of the porcelain to the metallic framework. The high adhesion strength helps the bridge construction successfully to resist the chewing efforts applied in different directions.

## 5.1. STRENGTH CHARACTERISTICS OF DENTAL ALLOYS, MANUFACTURED USING ADDITIVE TECHNOLOGIES

The investigation of the strength characteristics of dental alloys produced using additive technologies was performed by testing the tensile strength of flat specimens (Fig. 5-1). Three groups of samples were used: 1) fabricated by conventional casting of Co-Cr *Biosil-F* alloy; 2) casting with 3D printed models from Co-Cr *i-Alloy* and Ni-Cr *Wiron light* alloy, and 3) manufactured by SLM of Co-Cr *Co212-f* alloy.

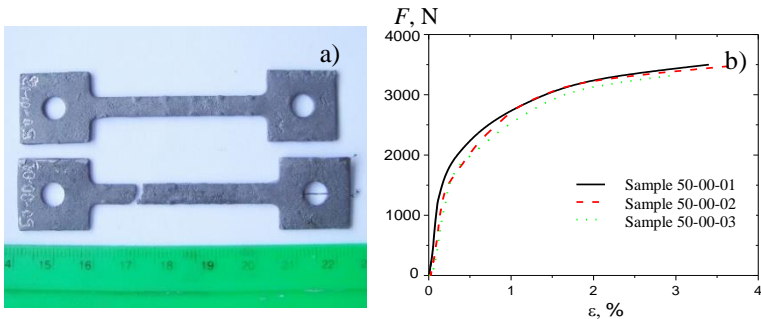


Fig. 5-1 Samples of Ni-Cr dental alloy *Wiron light*, cast with 3D printed patterns, before and after tensile test (a) and diagram load – deformation (b).

### 5.1.1. Strength characteristics of dental alloys, cast with 3D printed patterns

The experimental study has shown that the experimental values of the strength characteristics of all alloys tested, regardless of their production technology, are lower than those given by the manufacturer (Table 5-1), due to the different test conditions. In dental alloys, cast conventionally with wax or with 3D printed plastic patterns, there is no great difference in the strength properties.

### 5.1.2. Strength characteristics of dental alloys, produced by SLM

Co-Cr dental alloy *Co212-f*, manufactured by SLM, is characterized by increased strength properties - yield strength and

Table 5-1  
Mechanical properties of the investigated dental alloys.

Alloy	Type	Manufacturer's data					Research data				
		Rm	R <sub>0.2</sub>	E	Hardness		Rm	R <sub>0.2</sub>	E	Hardness	
		MPa	MPa	GPa	HV10	HRC	MPa	MPa	GPa	HV0.1	HRC
Wiron light (Bego), cast with 3DPP	Ni-Cr	880	470	200	260	-	453	272	191	-	-
i-Alloy (i-Dental), cast with 3DPP	Co-Cr	850	-	230	370	-	606	467	182	-	-
Biosil-F (Degudent) cast conventionally		900	700	220	400	-	-	410	209	335	33
Co212-f ASTM F75, SLM		1050	835	-	-	35	-	720	213	382	39

Note: 3DPP – 3D printed patterns

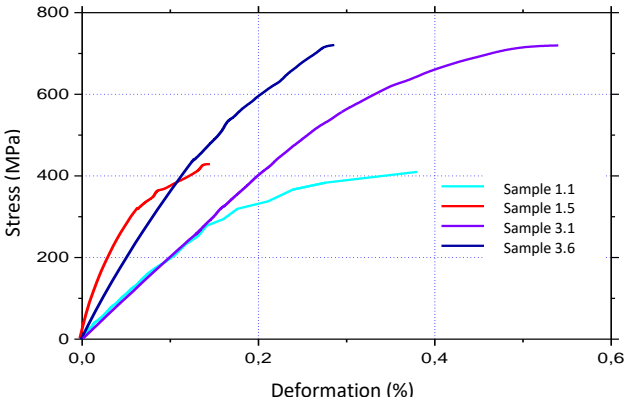


Fig. 5-2 Stress-strain diagram of Co-Cr dental alloys, manufactured conventional casting and SLM, with and without porcelain coating.  
 Sample 1.1 – cast Biosil-F alloy without coating;  
 Sample 1.5 - cast Biosil-F alloy with coating;  
 Sample 3.1. – SLM Co212-f alloy without coating;  
 Sample 3.6. – SLM Co212-f alloy with coating.

modulus of elasticity (Fig. 5-2) as compared to a cast *Biosil-F* alloy due mainly to the specific fine microstructure and the increased  $\epsilon$ -phase content of the SLM alloy. The modulus of elasticity of the SLM Co-Cr alloy *Co212-f* is 213 GPa and the yield strength  $R_{0.2} = 720$  MPa, which is 43% higher than the value of the conventionally cast alloy

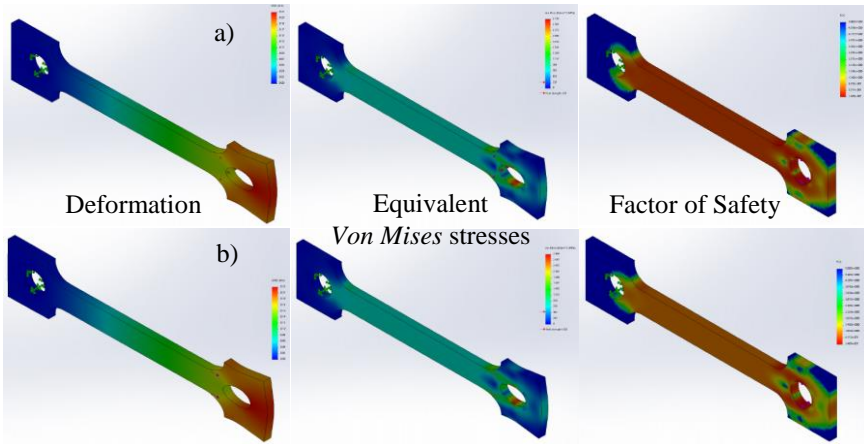


Fig. 5-4 Deformations, equivalent Von Mises stresses and FOS of Co-Cr samples, produced by casting (a) and SLM (b).

and meets the requirements of ISO 22674: 2016 standard, developed for dental restorations (> 500 MPa).

The simulation analysis of samples of Co-Cr dental alloys - conventionally cast *Biosil-F* and SLM *Co212-f* (Fig. 5-4) proved that the largest equivalent stresses occur at the end of the experimental area and close to the holder. This is why most of the samples were destroyed in this area, regardless of the production technology. Due to the close elastic modulus of the two Co-Cr dental alloys, there is not big difference in the deformation and distribution of equivalent stresses. The only difference is in the factor of safety (FOS). It is larger for the SLM *Co212-f* alloy due to the higher tensile strength.

## 5.2. ADHESION STRENGTH OF COATINGS ON DENTAL ALLOYS, MANUFACTURED USING ADDITIVE TECHNOLOGIES

In the present work, an experimental study of the adhesion strength of porcelain and composite coatings to Ni-Cr and Co-Cr dental alloys was performed for the first time by tensile tests. Specimens of the same shape and sizes were used, allowing not only to compare qualitatively the adhesion strength of the coatings but also to quantify the destructive stresses that cause their fracture. Compared

to ISO Standard 9693-1: 2012, the approach used makes it possible to determine the adhesion strength not only of porcelain but also of composite coating. The obtained results were processed by regression analysis and numerical modeling by finite element analysis (simulation analysis). The failure mode of the porcelain coating has been assessed according to a developed improved methodology.

### 5.2.1. Adhesion strength of coatings to dental alloys, cast with 3D printed patterns

#### 5.2.1.1. Adhesion strength of porcelain coating to Ni-Cr dental alloys, cast with 3D printed patterns

The adhesion strength of porcelain coating to dental alloys, cast with 3D printed patterns, was investigated using flat specimens of Ni-Cr alloy *Wiron light* (Fig. 5-5). Their casting models were made of *NextDent Cast* plastic by 3D printing at different slope ( $0^\circ$ ,  $45^\circ$  and  $90^\circ$ ) to the base using *RapidShape D30* stereolithographic printer.

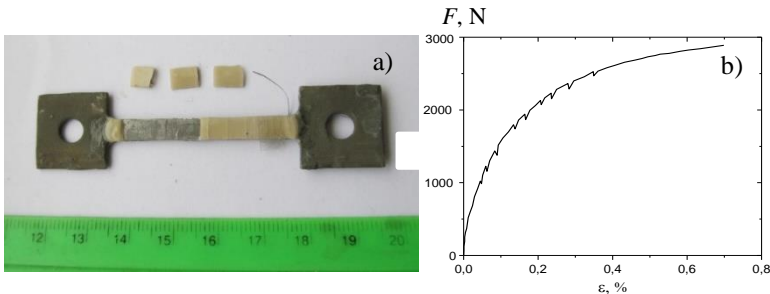


Fig. 5-5 Sample of Ni-Cr dental alloy *Wiron light* with porcelain coating after tensile test (a) and its diagram load-deformation (b).

It has been established that the adhesion strength of the porcelain coating to Ni-Cr alloys, cast with 3D printed patterns, is higher than those of cast by conventional technology. Depending on the regimes of 3D printing of cast patterns, the adhesion strength of the porcelain coating to the Ni-Cr alloy *Wiron light* varies from 63.4 MPa to 84.6 MPa.

A regression analysis of the results of the measurements of the mean arithmetic deviation  $Ra$  of the roughness of the Ni-Cr alloy and

the adhesion characteristics of the ceramic coating was carried out. Regression equations (13) and (14) were obtained to determine the influence of the technological factors  $X_1$  - layer thickness,  $X_2$  - the inclination angle of 3D printing on the roughness ( $R_a$ ) and the adhesion strength of the coating ( $\tau$ ).

$$Ra = 2.72833 + 0.26833X_1 + 0.2175X_1X_2 - 0.6975X_2, \quad (13)$$

$$\tau = 73.533 + 2.333X_1 + 3.525X_2 + 4.575X_1X_2, \quad (14)$$

Where:  $X_1$  – layer thickness and  $X_2$  – inclination angle of 3D printing.

On the basis of the experimental study for determining the adhesion characteristics of the ceramic coating, the maps of adhesion

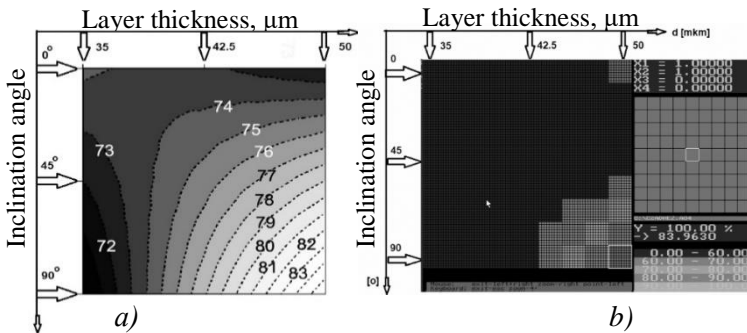


Fig. 5-6 Distribution of adhesion strength in samples with porcelain coating, represented by Mathcad software in MPa (a) and MADMML software in % (b).

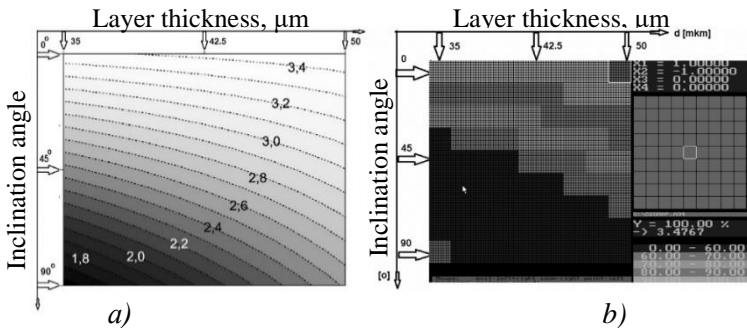


Fig. 5-7 Distribution of the mean arithmetic deviation of the roughness  $R_a$  in samples with porcelain coating, represented by Mathcad software in  $\mu\text{m}$  (a) and MADMML software in % (b).

strength distribution ( $\tau$ ) (Fig. 5-6) and the mean arithmetic deviation  $Ra$  of the roughness (Fig. 5-7) depending on the technological parameters were done using the *Mathcad* and *MADMML* software.

A multicriterial optimization on the adhesion strength and surface roughness criteria was performed for the first time. Multicriterial optimization allowed two regimes of 3D printing of cast

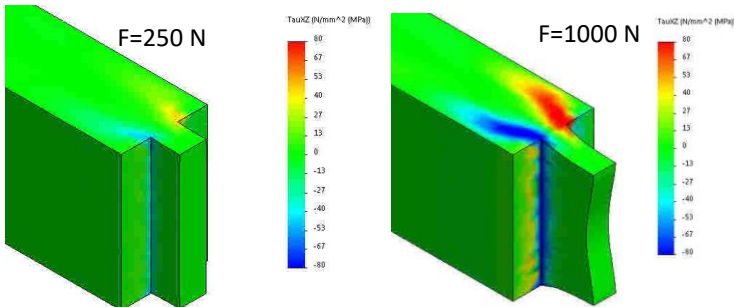


Fig. 5-8 Magnitude and distribution of shear stresses in load increase.

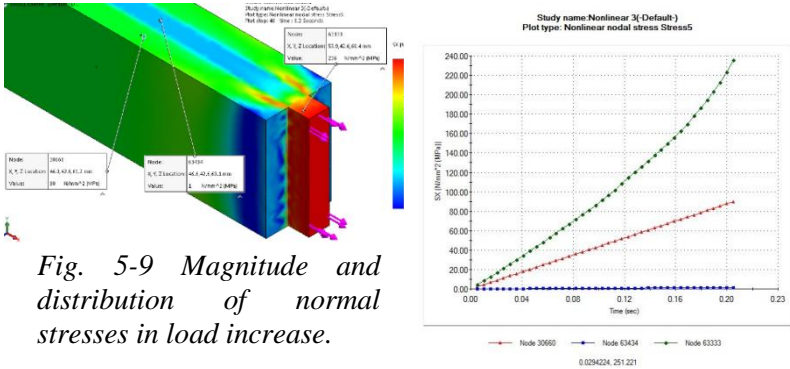


Fig. 5-9 Magnitude and distribution of normal stresses in load increase.

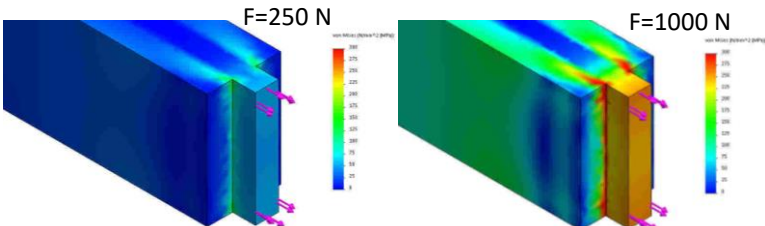


Fig. 5-10 Magnitude and distribution of equivalent von Mises stresses in load increase.

patterns to be obtained (layer thickness 50  $\mu\text{m}$ , slope angle of 56.3  $^\circ$  and 67.5  $^\circ$ ) in which maximum adhesion is resulted - 77.9 MPa and 79.9 MPa respectively.

The numerical modeling of the process gave an adequate explanation of the adhesive-cohesive mode and the sequence of the porcelain failure from the Ni-Cr alloy, cast with 3D printed models. The analysis showed that maximum normal, shear and equivalent stresses are generated along the coating/metal boundary at the free end of the coating (Fig. 5-8, Fig. 5-9 and Fig. 5-10). In this area, initially, the fracture of the coating starts by adhesive mechanism. The cohesive fracture of the coating begins at a certain distance from its free end with increase of the load at a later stage. With a further load increase, a mesh of cracks gradually originates in the coating until its final destruction from the base.

### 5.2.1.2. Adhesion strength of composite coating to Co-Cr dental alloys, cast with 3D printed patterns

Since the investigations have shown that the metallic specimens, cast with models printed with 50  $\mu\text{m}$  layer thickness, are characterized with highest values of the adhesion strength of the porcelain coating, the Co-Cr specimens whose models are printed with the same layer thickness are used for study the adhesion strength of composite coating.

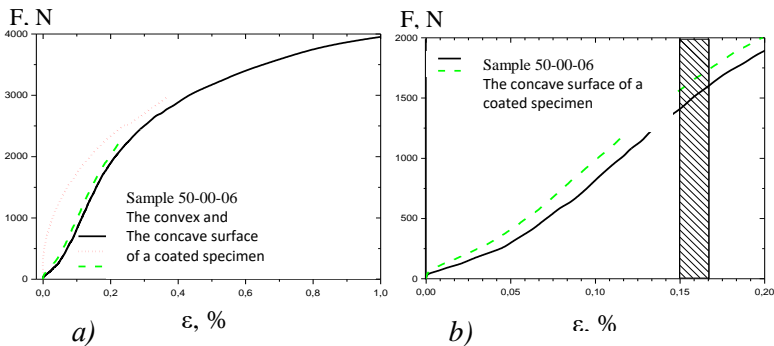
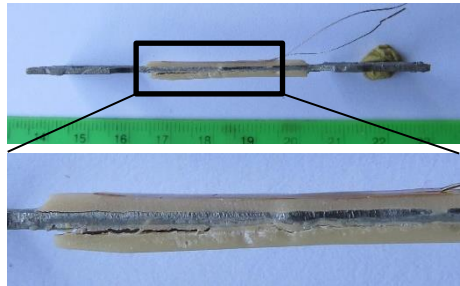


Fig. 5-11 Deformation curves of uncoated sample (50-00-06) and sample with composite coating (3D printing: 50  $\mu\text{m}/0^\circ$ )

In the present work, the elasticity modules of porcelain and composite (Fig. 5-11) are determined for the first time in tensile tests. The elasticity modulus of composite *Crea.lign set 12* is 8.5 GPa which is 7 times less than that of dental porcelain ( $E = 63\text{-}72$  GPa).

The adhesion strength of the composite coating to the Co-Cr dental alloy cast with 3D printed patterns is 13.5 - 19.5 MPa, i.e. about 4.5 times lower than the adhesion of a ceramic coating. Therefore, the roughness of the Co-Cr dental alloy, cast with 3D printed models, does not affect the adhesion strength of the composite coating.

The failure mode of the composite coating differs from that of ceramics. The composite coatings are delaminated from the metal surface without cracking (Fig. 5-12), i.e. their fracture mode is adhesive without a cohesive component.



*Fig. 5-12 Delamination of the composite coating in tensile test.*

### **5.2.2. Adhesion strength of porcelain coating to Co-Cr dental alloys, produced by SLM**

In the present study, the adhesion strength of porcelain coating on Co-Cr dental alloy *Co212-f*, produced by SLM, was investigated by tensile test. A comparative analysis with the values of the cast *Biosil-F* alloy was done. The results obtained based on two types of samples - with and without ceramic coating are presented in the diagram on Fig. 5-2. The calculations show that the adhesion strength of the porcelain coating to the SLM *Co212-f* alloy has a higher value than that of the cast *Biosil F* alloy - 83.1 MPa and 67.5 MPa respectively.

The fracture of the porcelain coating from the substrate made of *Co212-f* alloy by SLM under tensile test is shown on Fig. 5-13. During the test, multiple cracks, perpendicular to the direction of the applied force, is initiated in the porcelain coating at first. After that, with the load increase, the coating is destroyed at a critical crack distance of 1–2 mm, i.e. cohesion failure occurs, and finally it is delaminated from

the substrate The observation of the sample's surface has shown that the coating does not completely detach from the metallic substrate. More than 50% of the surface area of the SLM alloy is covered by porcelain residues of the opaque layer. Their distribution is comparatively homogeneous with larger quantity in the sites of the cracks initiation. The investigation with high magnification confirmed that the higher surface roughness ( $R_a=5.89\ \mu\text{m}$ ) of the SLM samples is due to the specific morphology, characterizing with traces of the building layers and tracks and the presence of partially melted powder particles as well (Fig. 5-13-a). It can be clearly seen that the partially melted powder particles act as a retention sites, holding larger quantity

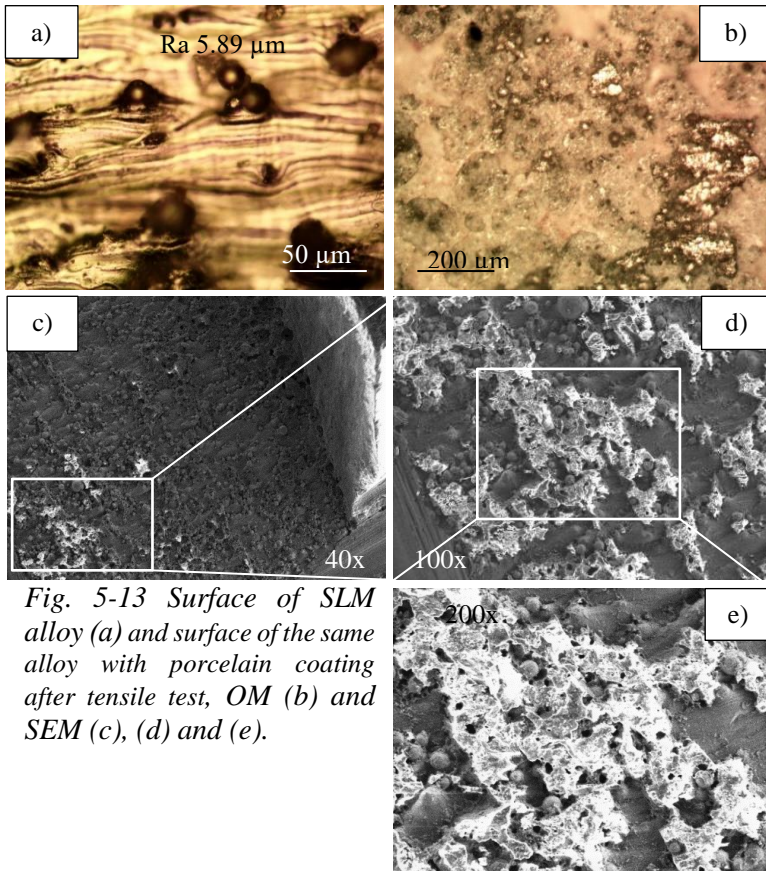


*Fig. 5-13 Surface of SLM alloy (a) and surface of the same alloy with porcelain coating after tensile test, OM (b) and SEM (c), (d) and (e).*

of porcelain remnants on the surface of the SLM alloy (from Fig. 5-13-b to Fig. 5-13-e).

The failure of the porcelain coating on the sample of cast *Biosil-F* alloy is similar except that the critical step of the cracks is greater - 4-6 mm. After the tests, less than 50% of the surface of the cast samples is covered with porcelain residues with uneven distribution. It can be seen on Fig. 5-14-a that the surface roughness of the sandblasted cast alloy ( $R_a=2.67\ \mu\text{m}$ ) is lower than the SLM sample. As a result, large areas with no porcelain residues exist on the sample's surface after the experiment (Fig. 5-14-b). The SEM study showed that the porcelain was completely "detached" from the metal base (Fig. 5-14-c and Fig. 5-14-d). The irregular porcelain residues are evidence of uneven adhesion of ceramics to the cast alloy.

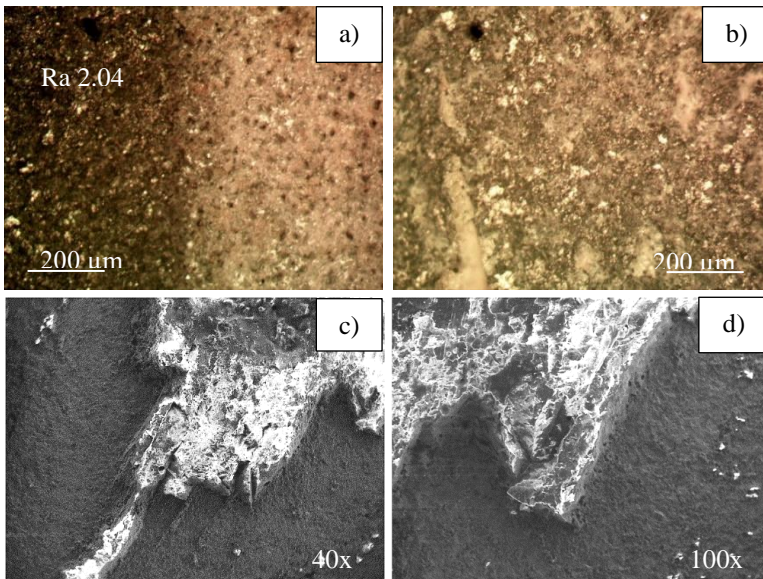
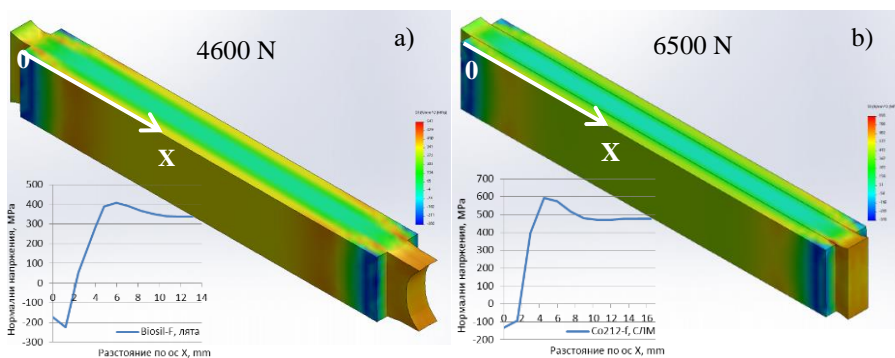


Fig. 5-14 Surface of cast *Biosil F* alloy with porcelain coating before (a) and after tensile test (b), (c) and (d) (OM (a), (b) and SEM (c), (d)).

The smaller critical crack distance in the coating and the higher quantity of the porcelain residues on the surface of the SLM alloy after tensile test indirectly indicate higher bond strength of the porcelain coating compared to the cast alloy, which is proven by the calculations.

In metal-ceramic restorations the bond strength of the porcelain coatings to dental alloys depends on the mechanical interlocking of the opaque layer on the rough metal surface, chemical bond between the oxide layer of the metal substrate and the ceramic as well as the coefficients of thermal expansion of both materials – the porcelain and the alloy. Among these three factors, the chemical component exerts main impact on the porcelain-alloy bond strength. In our experiment as-received SLM Co-Cr substrate is used with about 3 times higher roughness compared to the cast. The surfaces of the SLM samples are characterized with traces of the building layers and tracks as well as presence of partially melted powder particles. Therefore, the first opaque layer can penetrate deeper in the surface voids, grooves and gaps between the layers, resulting in better mechanical interlocking. From the other hand, the higher surface roughness of the SLM substrate ensures larger area for chemical interaction with the ceramic compared to the cast and sandblasted. As a result, the adhesion strength of the porcelain coating to the as-received SLM Co-Cr dental alloy is higher than the cast one. When the adhesive bonding force between the alloy and the ceramic is higher than the ceramic cohesive forces, then the cohesive failure can be expected [Chang H.S. et al. (2016)]. Therefore, the higher bond strength of the porcelain coating to the SLM Co-Cr alloy is the main reason for predominantly cohesive fracture mode, evaluated on the improved criterion ((p.2.5.1. chapter



*Fig. 5-17 Normal stresses in Co-Cr samples with two-sided porcelain coating, manufactured by casting (a) and SLM (b).*

2) as mixed/cohesive. While the lower adhesion strength of the ceramic to the cast alloy leads the mixed/adhesive failure mode.

Data of the simulation analysis gives an adequate explanation about the failure mechanism of the porcelain coating. The simulation analysis has shown identical distribution of normal, shear and equivalent stresses in the samples from both alloys – cast *Biosil-F* and SLM *Co212-f* (Fig. 5-17, Fig. 5-19, Fig. 5-20, Fig. 5-21). The only

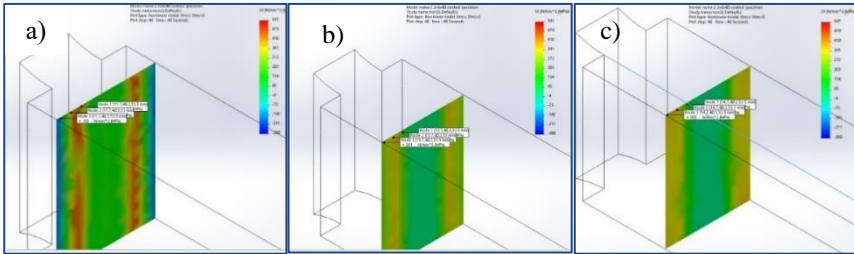


*Fig. 5-19 Distribution of the normal stresses in different cross sections of sample, cast of Co-Cr Biosil-F alloy, with two-sided porcelain coating.*

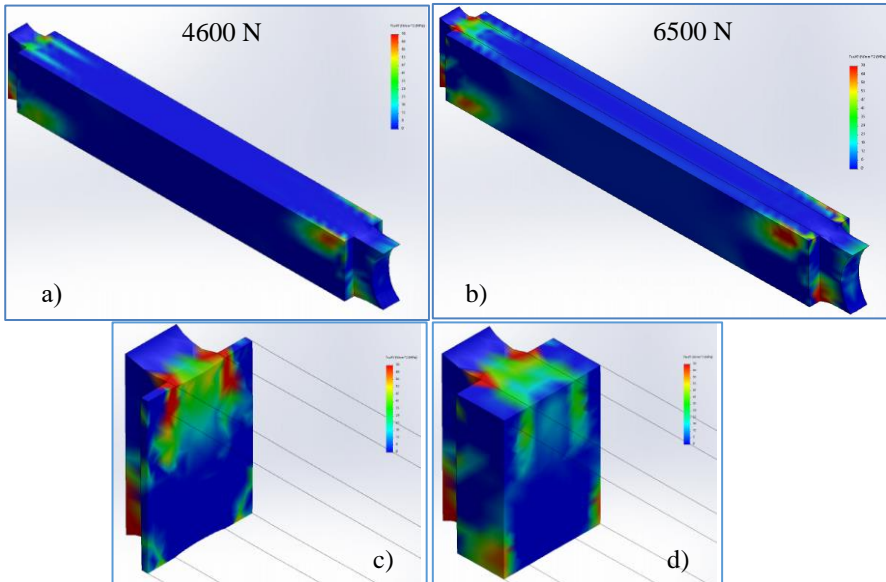


*Fig. 5-20 Shear stresses in Co-Cr samples with two-sided porcelain coating, manufactured by casting (a) and SLM (b), (c) and (d).*

difference is in the magnitude of the stresses, which are higher for the SLM alloy. This indicates failure of the coating in higher loading that is revealed by the experimental results. Because of maximum shear and normal stresses are at the porcelain-metal interface on the coating free edge, the porcelain fracture will start there – cohesively by cracking of the ceramics or adhesively by delamination from the metal substrate. As the adhesion strength of the porcelain coating to the cast

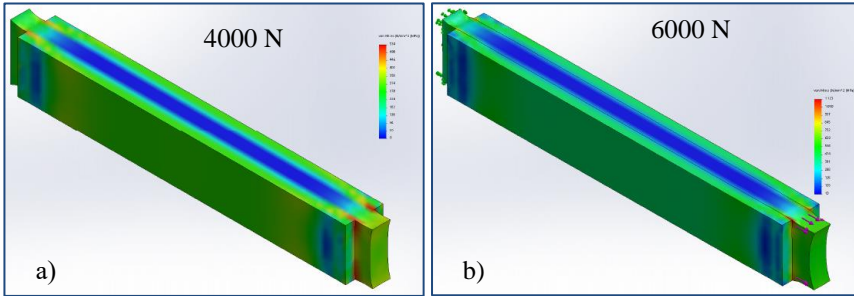


Fig. 5-21 Equivalent von Mises stresses in Co-Cr samples with two-sided porcelain coating, manufactured by casting (a) and SLM (b).

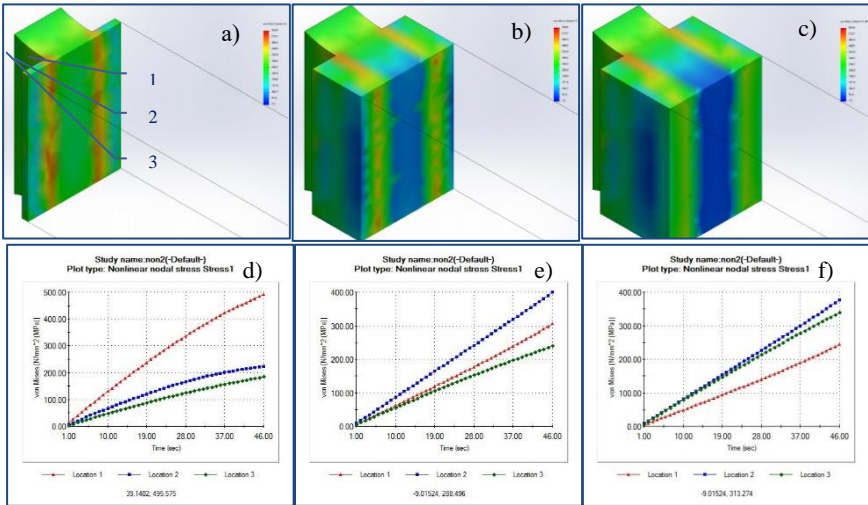


Fig. 5-23 Distribution of the equivalent Von Mises stresses in cross sections of sample, cast of Co-Cr Biosil-F alloy, with two-sided porcelain coating (a), (b), (c). (4600 N load). Change of the equivalent Von Mises stresses in different points of the porcelain coating (d), (e) and (f).

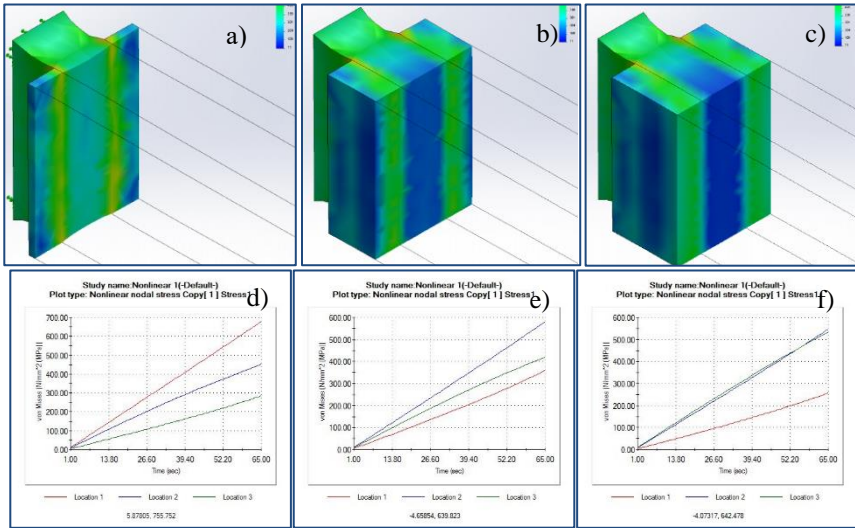


Fig. 5-30 Distribution of the equivalent Von Mises stresses in cross sections of SLM sample of Co212-f alloy with two-sided porcelain coating (a), (b), (c). (6500 N load). Change of the equivalent Von Mises stresses in different points of the porcelain coating (d), (e) and (f).

alloy is lower, its failure will start adhesively. The higher bond strength of the ceramic to the SLM alloy will determine cohesive start of the fracture. Due to change of the location of maximum stresses from the coating free edge through its thickness to the surface (Fig. 5-19, Fig. 5-23 and Fig. 5-30), the destruction is cohesive. The sample, shown on Fig. 5-31, has failed the similar mode, confirming the adequacy of the simulation model used.

The identical stresses distribution defines mixed failure mode of the porcelain coating on the cast and SLM Co-Cr dental alloys upon tensile test. The bond strength of the ceramic to the alloys determines if it is

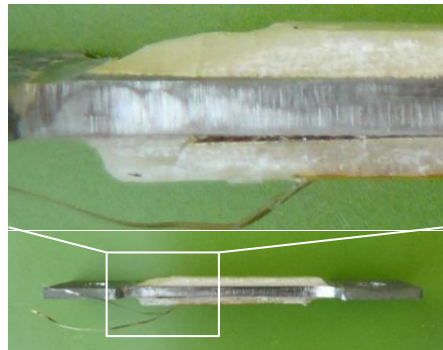


Fig. 5-31 Sample after tensile test with fractured porcelain coating (SLM Co212-f alloy).

predominantly cohesive or adhesive. Due to the higher adhesion strength of the ceramic to the SLM alloy the fracture mode of the coating is mixed/cohesive, while in the cast alloy it is mixed/adhesive. It should be noted that the higher roughness of the as-received SLM Co-Cr samples is one of the main factors, defining the higher bond strength and the mixed/cohesive failure mode of the porcelain coating.

As for successful clinical application of the metal-ceramic FPDs the cohesive failure mode is preferred, the SLM process appears a very promising alternative for manufacturing of metal frameworks.

### 5.3. BENDING STRENGTH OF DENTAL ALLOYS, MANUFACTURED USING ADDITIVE TECHNOLOGIES

The bending strength of dental alloys has been investigated by a newly developed methodology involving experiment and numerical

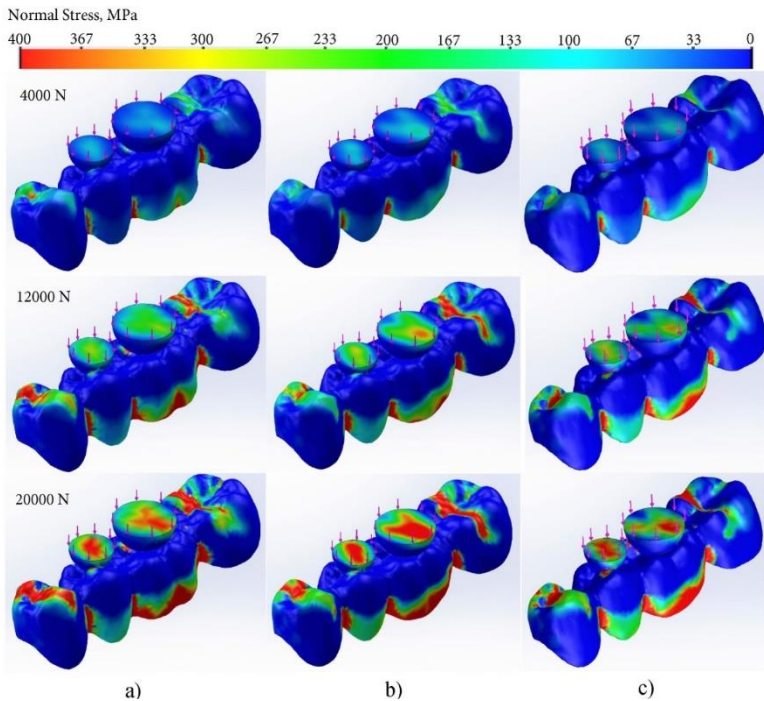


*Fig. 5-32 Change of normal stresses with loading increase in bending test simulation of Co-Cr dental bridges: (a) conventionally cast sample; (b) sample cast with 3D printed pattern and (c) SLM sample.*

modeling using engineering CAD software. Four-part bridges from 1-st premolar to the 2-nd molar are used, fabricated of Co-Cr alloys by conventional casting, casting with 3D printed patterns and SLM. The methodology has been developed in such way that during the experiment the loading of the bridges is applied as close as possible to the actual.

The simulation of the four-point bending test of virtual models of real bridges has shown that the highest normal stresses are located in the cervical areas of the pontics and the connectors (Fig. 5-32). The distribution of the normal and equivalent *Von Mises* stresses as well as deformations for Co-Cr dental alloys fabricated by the three technologies do not differ significantly (Fig. 5-33 and Fig. 5-34).

Investigation the normal stresses at critical points on the vestibular surface of the most loaded sections has shown that they are changed with different intensity (Fig. 5-38). For the conventionally cast sample (Fig. 5-38-a), the stresses in the connector between the two premolars are highest, followed by the connector between the two molars and finally those in the connector between the second premolar

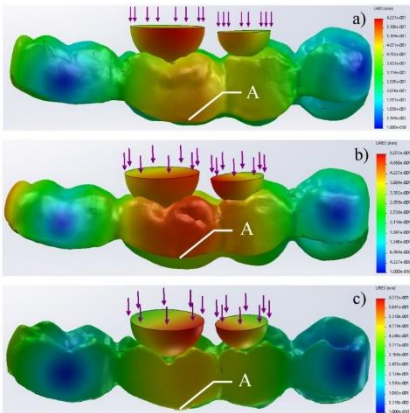


Fig. 5-33 Maximal displacement in bending test simulation of Co-Cr dental bridges: conventionally cast sample (a), sample cast with 3D printed pattern (b) and SLM sample (c). (Loading 20 000 N).

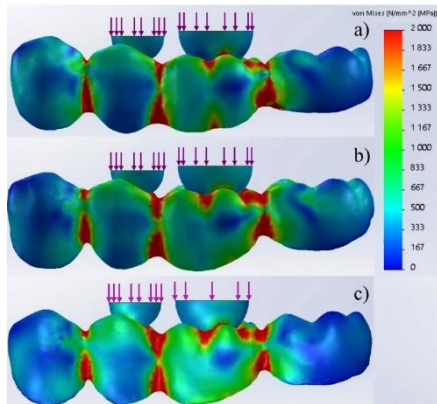


Fig. 5-34 Von Mises stresses in bending test simulation of Co-Cr dental bridges: conventionally cast sample (a), sample cast with 3D printed pattern (b) and SLM sample (c). (Loading 20 000 N).

and the first molar (pontics). In the specimen, cast with 3D printed pattern (Fig. 5-38-b), there is a difference in the stresses distribution. The highest stresses are in the connector between the two molars, followed by the connector between the pontics and finally that of the connector between the two premolars. This means that it is expected initiation of crack at first in the connector between the two molars and then between the pontics. The difference in the distribution of normal stresses for both types of samples is due to the different cross-sectional areas of the most loaded sections. In the bridge, cast with 3D printed pattern, the cross section between the two molars has a 3.5 mm<sup>2</sup> area

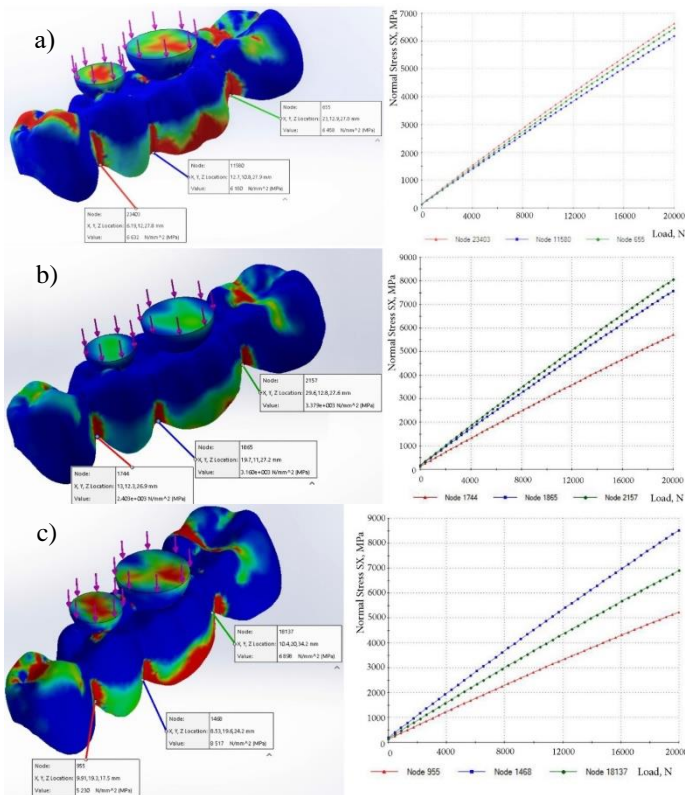


Fig. 5-38 Changes of normal stress at critical points of dental bridges during simulation of bending test: conventionally cast sample (a), sample, cast with 3D printed pattern (b) and sample, manufactured by SLM (c).

less than the same section of the conventionally cast bridge. For this reason, the highest stresses are concentrated in this zone and the first crack appears. During the tests, the actual bridge was destroyed exactly this way - first between the two molars and then between the bridge bodies.

The tendency of change the normal stresses at critical points of the most loaded sections is very pronounced in the SLM bridge (Fig. 5-38-c). In this case, the stresses in the connector between the two pontics are highest, followed by the connector between the two molars and finally that of the connector between the two premolars. Therefore, the fracture is expected to occur in the section with the highest stresses – connector between the two bridge bodies.

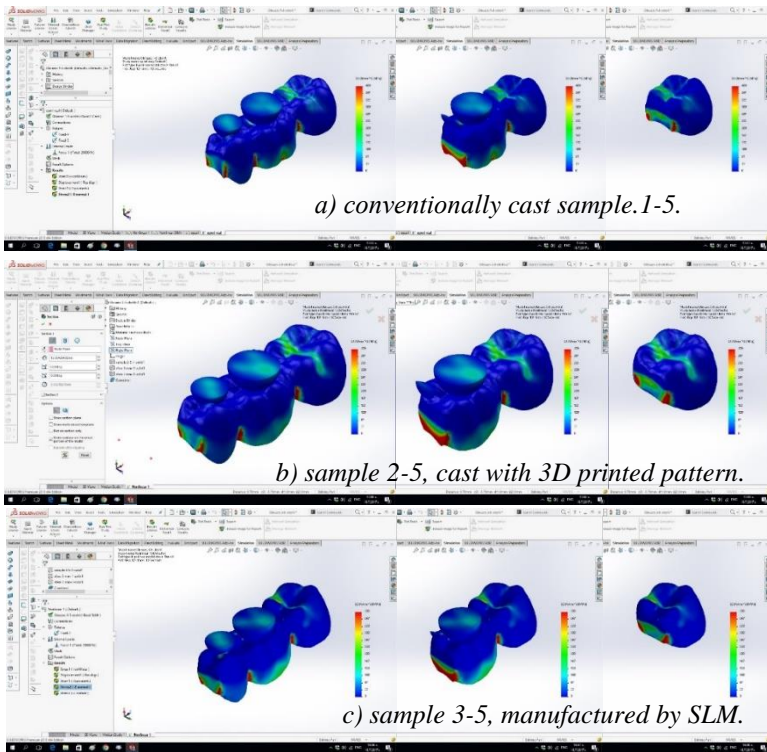


Fig. 5-40 Normal stresses in the connectors between pontics in 4000 N loading.

Analysis of the normal stresses distribution in the section between second premolar and first molar (Fig. 5-40) gave an answer to the question why the most samples were destroyed between the pontics during the experiment. During bending process of dental bridges, produced by the three technologies, the highest stresses were concentrated at the lower part of the cross section of the connector between the pontics.

The experimental study confirmed the results of the simulation analysis. Almost all bridge constructions were destroyed at the connector between the two pontics during bending test. The possibility to predict the sites and sections, at which the rupture of the samples could be expected, has proven the adequacy of the simulation model.

During the experiment, it was found that the destruction of the cast Co-Cr dental bridges consists of three stages - crack initiation in the area with the highest loading, its development and fracture of the construction (Fig. 5-35). The appearance of the crack was fixed on the diagrams of samples 1-2 and 2-2 by a sharp reduction of the load (Fig. 5-36). The appearance of the crack occurs at very close average loads: 9.820 kN in conventionally cast bridges and 10.171 kN in cast with

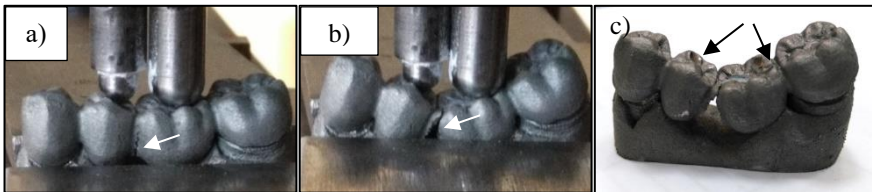


Fig. 5-35 Process of bending of cast dental bridge (a) and (b) and destroyed bridge (c).

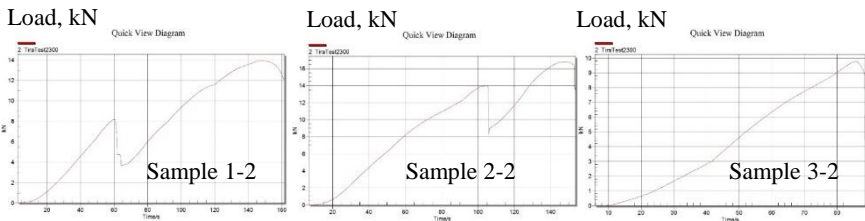


Fig. 5-36 Diagrams in bending test of Co-Cr dental bridges. (Sample 1-2 - conventionally cast with wax pattern, sample 2-2 - cast with 3D printed pattern and sample 3-2 - produced by SLM).

3D printed patterns (Fig. 5-37). While the final destruction of the second group is at a higher load – 17.631 kN compared to the first – 14.097 kN. The greater bending strength of the bridges, cast with 3D printed patterns, is due to their higher strength, as evidenced by the hardness measurements.

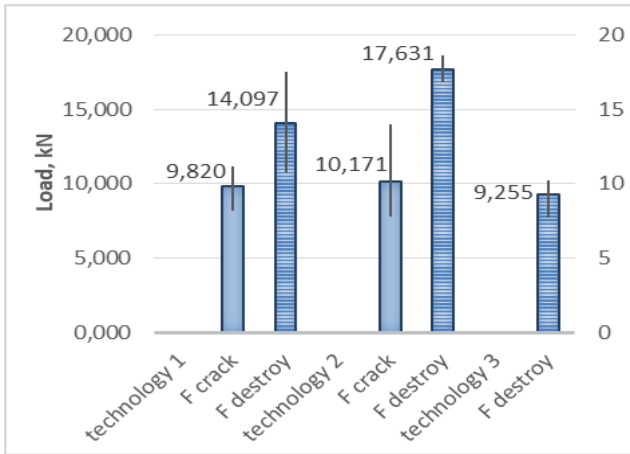
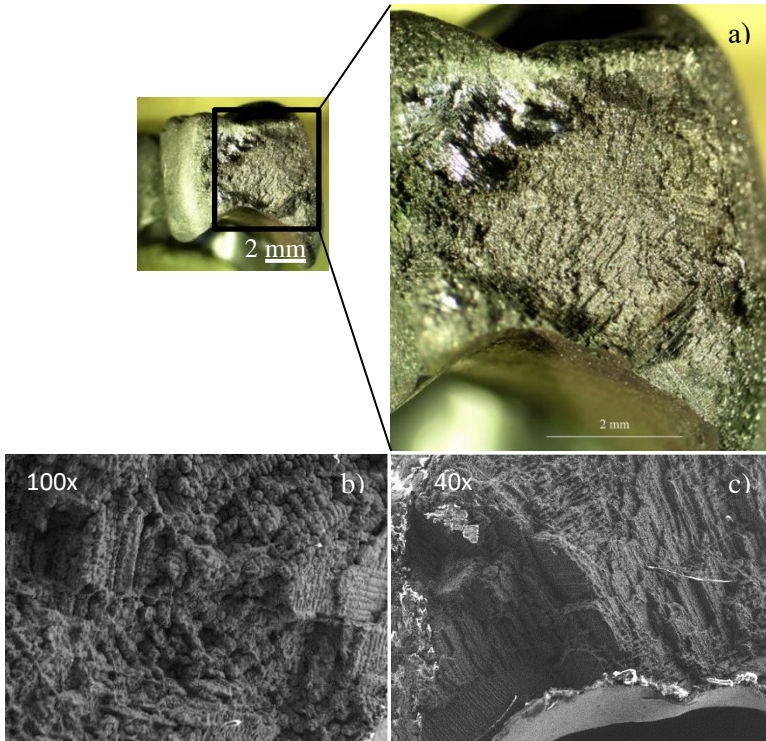


Fig. 5-37 Loadings of cracking and destroying of dental bridges during bending test. (Technology 1 – conventional casting with wax patterns, technology 2 – casting with 3D printed patterns and technology 3 – SLM).

During bending test, the SLM dental bridges were destroyed suddenly in the connector between the two bridge bodies without appearance and development of a crack, characteristic of the cast specimens. The diagram obtained during the experiment (Fig. 5-36, sample 3-2) is characterized by one peak of the load. The fracture occurred at a load of 9.255 kN, which was close but less than the loads in which the cast samples were cracked (Fig. 5-37). The comparative analysis of the geometric characteristics of the most loaded sections indicates that the cross-sectional area of the connector between the two pontics is the least for the SLM bridge

Since the hardness and yield strength of the bridges, produced by SLM, are larger than the cast ones and simulation analysis showed twice-larger reserve of strength, we expected that they would be

destroyed in much greater loading. Therefore, the most probable reason for their fracture in loading, in which a crack in the cast samples appears, is their porous structure and the smaller area of the most loaded section.



*Fig. 5-41 Fracture surface of conventionally cast sample.*

The investigation of the fracture surface of dental bridges (Fig. 5-41 and Fig. 5-42) confirmed further the simulation data. On the pictures of both cast samples, it is clearly visible the site of crack initiation and its development. The fracture character is typical for cast construction - intergranular with clearly visible traces of particular grains and dendrites. Based on the investigations of the microstructure and bending strength by tests and simulation analysis, a scheme of the mechanism of the crack originating and development during the fracture of cast Co-Cr dental alloys was made (Fig. 5-44).

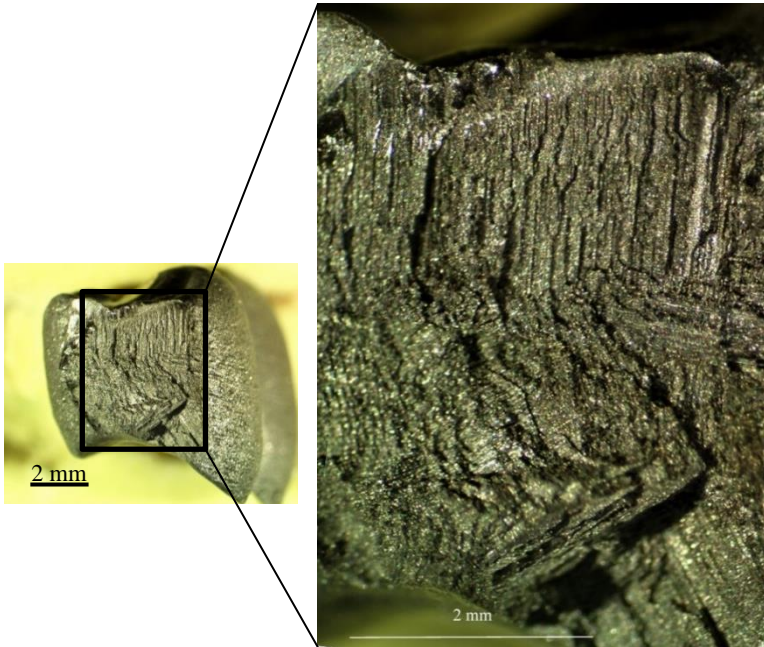


*Fig. 5-42 Fracture surface of sample, cast with 3D printed patterns.*

The specific layered macrostructure, the fine microstructure with dendritic morphology, the phase composition – the presence of  $\epsilon$ -phase and the typical defects of the SLM Co-Cr alloy *Co212-f* define the fracture mechanism during bending. In dental bridges, made by SLM, many pores with different sizes, poor welding between the separate layers and tracks as well as cracks between them were observed (Fig. 4-11, Fig. 5-54, Fig. 5-55-a and Fig. 5-55-b). At larger magnification of the fracture surface, the cracks, connecting the individual pores, are clearly visible (Fig. 5-55-c). Fig. 5-55-d shows the beginning of the cracks at the boundaries between the melted traces and layers. Consequently, the specific microstructure is a prerequisite for destroying the SLM bridges not by initiation and growth of single cracks but by generating and development of a network of cracks across the entire area of the most loaded section.

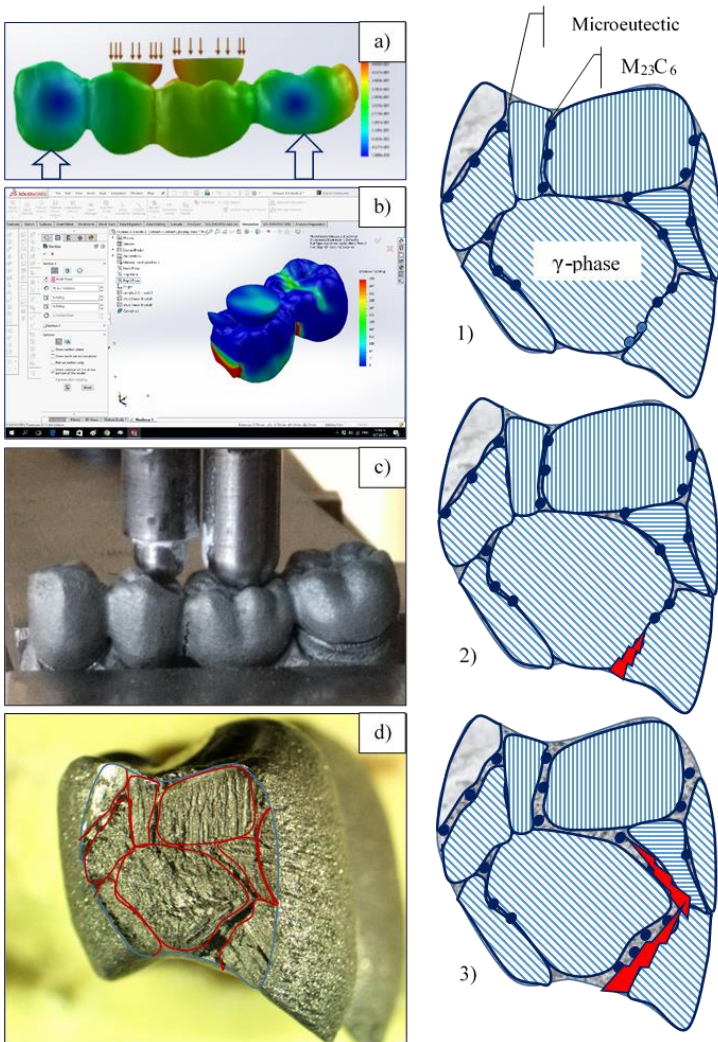


*Fig. 5-44 Dental bridge, cast of Co-Cr alloy. Loading scheme and deformations during bending (a), normal stresses in the most loaded cross section (b), crack initiation (c) and fractured surface of the bridge (d). Schemes of the microstructure of the cast Co-Cr dental alloy (1), crack origination and growth (2) and (3).*

Scheme of the fracture mechanism of dental bridge, made by SLM, is shown on Fig. 5-56. This mode of destruction is dangerous for constructions that work on a cyclical loading, such as fixed partial dentures. Therefore, prior to introduction of the SLM process for production of dental constructions, the technological regimes have to be optimized in order to obtain a dense structure without pores and defects.

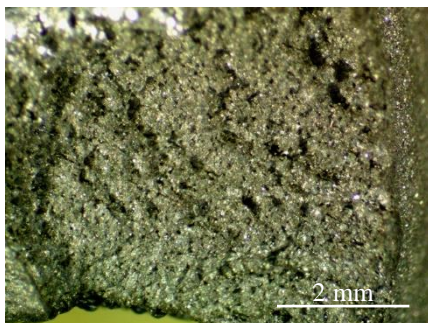


*Fig. 5-54 Fracture surface of SLM sample 3-2 (OM).*

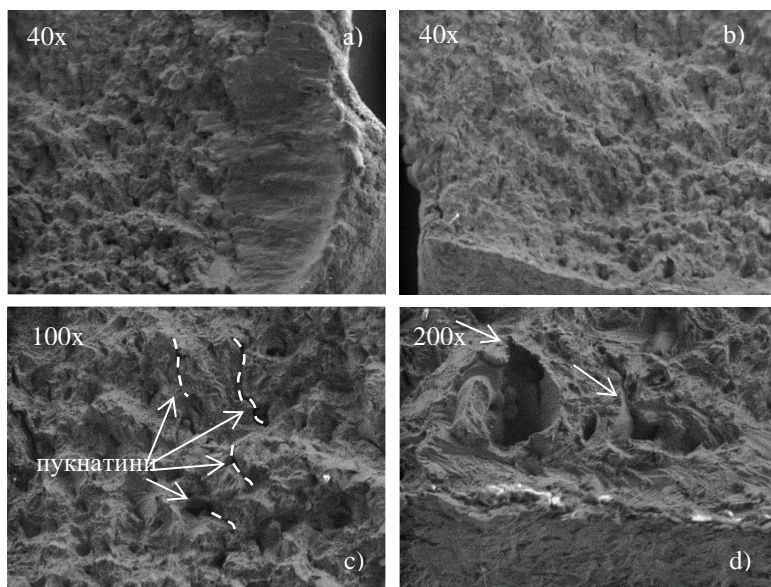


*Fig. 5-55 Fracture surface of SLM sample (SEM).*

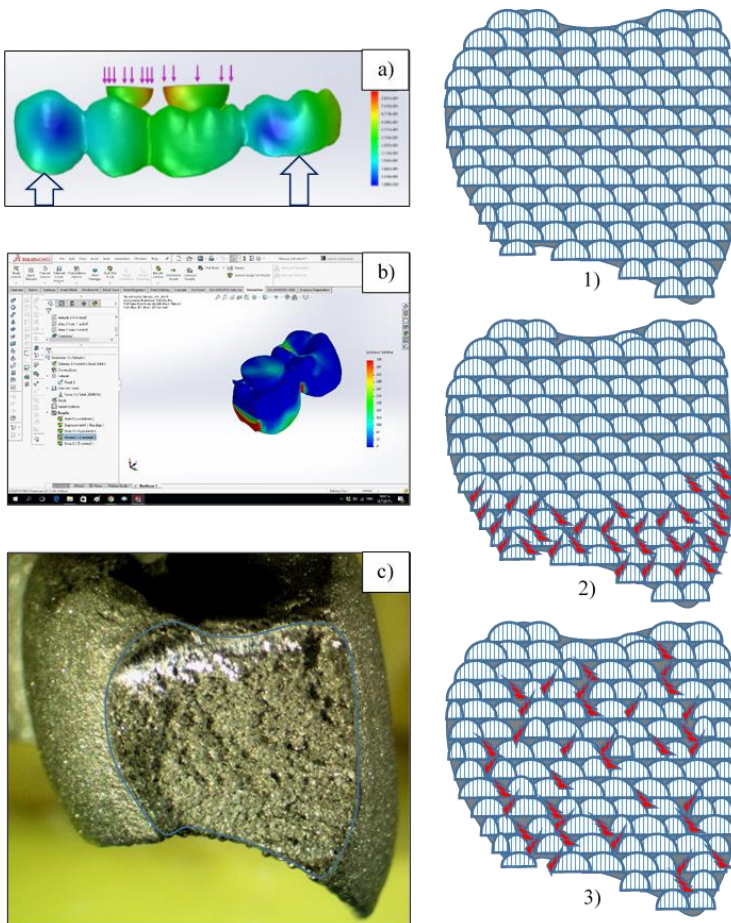


*Fig. 5-56 Co-Cr dental bridge, manufactured by SLM. Loading scheme and deformations during bending (a), normal stresses in the most loaded cross section (b) and fractured surface of the bridge (c). Schemes of the microstructure of the SLM Co-Cr dental alloy (1), origination and development of multiple micro-cracks (2) and (3).*

#### **5.4. TRIBO-CORROSION OF Co-Cr DENTAL ALLOYS, MANUFACTURED BY SLM**

In the present work, a study of the tribio-corrosive behavior in artificial saliva (*Fusayama-Meyer* solution) of two Co-Cr dental alloys - *Co212-f* and *Biosil-F*, manufactured by SLM and casting

respectively, was performed for the first time. Since the alloys are manufactured using different technologies, the microstructure of the cast and SLM samples differs significantly, which determines the different wear and corrosion properties.

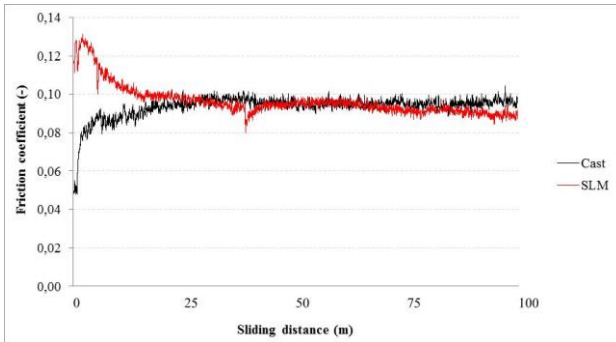


Fig. 5-57 Variation of COF values as a function of sliding distance.

The friction coefficients (COF) of the two alloys change in a different way during the experiment (Fig. 5-57). COF value of SLM alloy initially has its maximum value as 0.13 and then goes down during sliding. The COF of the cast alloy has a tendency to increase till the end of the running-in regime and it has a peak value of 0.09. At

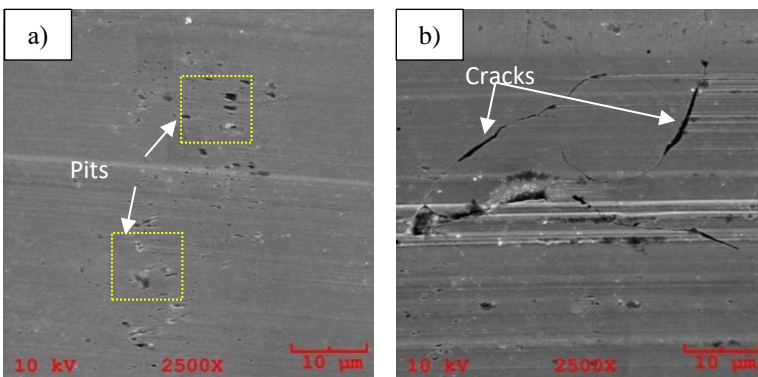
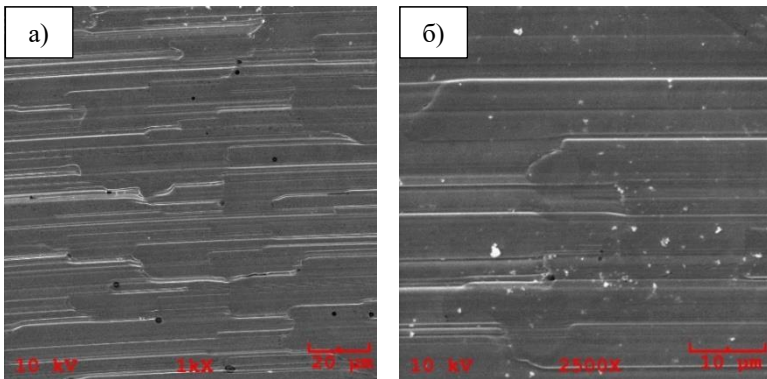


Fig. 5-59 SEM images showing several pits (a) and (b) cracking in adhered layer on the worn surface of tested cast alloy.

the steady-stage regime, the COF values of both alloys have no significant change and vary in the range of 0.08 – 0.10.

The examination of the worn surfaces reveals different wear types for the cast and SLM Co-Cr-Mo alloys. The worn surface of the cast alloy exhibits a very smooth wear track with many pits and cracks as well as a thick degraded film layer (Fig. 5-59). While the worn surface of the SLM alloy has very sharp plastic flows which are oriented step by step due to the alloy's layer-layer structure and also deep grooves exist indicating abrasion type wear (Fig. 5-60).



*Fig. 5-60 SEM images showing plastic flows on the worn surface of SLM processed alloy: (a) plastic flows which are oriented step by step due to layer-layer structure of tested alloy, (b) deep grooves indicating the abrasion type wear under studied conditions.*

Due to the more homogeneous microstructure, the higher hardness and the more stable oxide layer formed on the surface, the SLM processed alloy is more resistant to both corrosion and wear, thus proving that the SLM is a promising manufacturing method for dental applications.

## **SIXTH CHAPTER**

### **ADDITIVE TECHNOLOGIES IN PRODUCTION OF DENTAL CONSTRUCTIONS**

The research in the present work shows the advantages of the additive technologies, but also certain features of the constructions made with them, referring to the geometrical and surface characteristics, the microstructure, the mechanical and the tribo-corrosion properties. Based on the results obtained, particular stages and operations of the existing technologies were eliminated, improved or developed. The aim of the innovations is to obtain dental constructions with higher accuracy and mechanical properties. The attention is focused on the application of the additive technologies in the overall production process of fixed partial dentures.

#### **6.1. PRODUCTION OF TEMPORARY BRIDGES AND CROWNS WITH STEREOLITHOGRAPHY**

The high dimensional accuracy and fitting to the prepared teeth, as well as the high smoothness of the surfaces of the temporary crowns and bridges are of particular importance for their proper functioning. On the other hand, a technological process is effective, if it ensures fast production of the details.

It is established in the present study that for effective fabrication of provisional crowns and bridges with high dimensional accuracy and surface smoothness using *RapidShape D30* printer individual corrections of the dimensions along the separate axes of the virtual model has to be done. The corresponding correction coefficients, which depend on the construction type – crown or bridge, have been calculated and proposed. In order to ensure a relatively high surface smoothness, the construction should be positioned with vertical axes of the teeth parallel to the printing direction (Z-axis). The number of the supports has to be increased ( $\geq 4$  per tooth) for reduction of deformations during 3D printing and final photopolymerization.

The technological features and the algorithm for designing the virtual model and the fabricating process of temporary crowns and

bridges providing high accuracy and smoothness are summarized in Table 6-4.

*Table 6-4.*  
*Algorithm for design of virtual model and 3D printing process of temporary crowns and bridges with RapidShape D30 printer.*

Technological feature		Crown	Bridge construction
<b>3D printing process</b>			
Printer		<i>RapidShape D30</i>	
Polymer		<i>NextDent C+B</i>	
Layer thickness		50 μm (recommended by the producer)	
<b>Design of the virtual model</b>			
Position		Vertical axes of the teeth must be parallel to the printing direction Z-axes.	
Supports number		≥4	≥4 of each tooth
Corrections of the dimensions	Along axes X or Y	0%	An increase with 0.44% on the axis with the largest size; 0% on the other axis.
	Along axes Z	Decrease with 2%	
<b>Additional treatment</b>			
<i>Final photopolymerization</i>		The construction must be placed on a working model.	

## 6.2. FIXED PARTIAL DENTURES, MANUFACTURED BY CASTING WITH 3D PRINTED PATTERNS

The quality of Co-Cr dental alloys, cast with 3D printed patterns, is influenced by three groups of factors: the properties of the materials for 3D printing, the special features of the 3D printing process and the peculiarities of the casting.

When manufacturing cast patterns by 3D printing, certain dependencies must be observed to ensure production of quality castings. In 3D printing of the cast patterns, it is necessary to select the plastic intended for the corresponding application, which should burn without residue and have minimal or zero thermal expansion. The investment material for mold manufacturing must be selected depending on the polymer type of the cast patterns, while the heating regime of the casting mold should be determined by the type of investment material and the alloy to be cast.

The present study has shown that in order to obtain ceramic or metalceramic FPDs with high accuracy and adhesion strength of the porcelain coating using AT in their production, it is necessary to produce precise cast patterns by 3D printing, as the dimensions being corrected with the calculated and proposed coefficients on the virtual model stage.

It should be taken into account that the increased roughness of the 3D printed cast patterns is a disadvantage in dental constructions with high smoothness requirements and an advantage in metalceramic dental prostheses. Therefore, the position of the patterns relative to the printing direction should be different for FPDs of pressed ceramics and in casting frameworks of dental alloys for metalceramics. In the first, the vertical axes of the teeth must be parallel to the built direction of the Z-axis, and in the second, they should be inclined at an angle of 45° to 70° to the base.

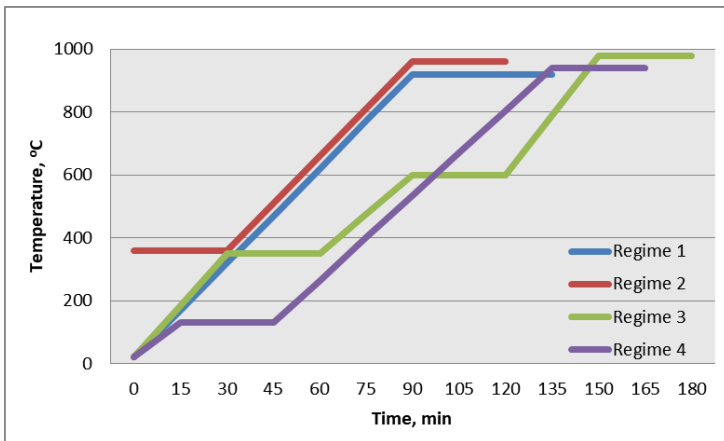


*Fig. 6-4 Heating regimes of the casting mold: Regime 1 – investment material Sherafina-Rapid, conventional casting with wax pattern; Regime 2 – investment material Sherafina-Rapid, casting with polymer patterns; Regime 3 - investment material Sherafina-Rapid, Ni-Cr alloy Wiron-light, casting with 3D printed patterns of the polymer Nextdent Cast; Regime 4 - investment material Sheravest RP, Co-Cr alloy i-Alloy, casting with 3D printed patterns of the polymer Nextdent Cast.*

When manufacturing the casting mold with the widely used *Sherafina-Rapid* investment material, it is necessary the heating to be performed using the newly developed isothermal regime (Fig. 6-4), which guarantees the quality casting.

It is proposed for the first time *not to apply operations for increasing the surface smoothness* of the 3D printed cast patterns in

Table 6-5  
Technological processes for manufacturing of fixed partial dentures by metal casting or ceramic pressing with 3D printed patterns.

Technological feature		Crown	Bridge
<b>3D printing process</b>			
Printer		<i>RapidShape D30</i>	
Polymer		<i>NextDent Cast</i>	
Layer thickness		50 μm (recommended by the producer)	
<b>Design of the virtual model</b>			
Position		<b>Casting of dental alloys</b>	
		Vertical axes of the teeth must be inclined at 45°-70° towards the base.	
		<b>Ceramic pressing</b>	
		Vertical axes of the teeth must be parallel to the printing direction Z-axes.	
Supports number		≥4	≥4 of each tooth
Corrections of the dimensions	Along X or Y axes	0%	An increase with 0.50 % on the axis with the largest size; 0% on the other axis.
	Along Z axis	Decrease with 2%	
<b>Additional treatment</b>			
<i>Final photopolymerization</i>		The construction must be placed on a working model.	
Increasing surface smoothness.		<b>Casting of metal framework for metalceramic FPDs: NOT APPLICABLE</b> <b>Ceramic pressing:</b> Cover with thin wax layer or treatment with solvent.	
<b>Manufacturing of casting mold (casting of dental alloys)</b>			
Investment material		<i>Sherafina-Rapid</i>	<i>Sheravest RP</i>
Heating regime of the casting mold		<b>Newly proposed regime:</b> Start: 22 °C – room temperature ↑9 °C/ min Hold 30 min at 350°C ↑9 °C/ min Hold 20min at 600°C ↑9 °C/ min Hold 30min at 980°C	<b>From the manufacturer:</b> Start 22 °C – room temperature ↑9 °C/ min Hold 30 min at 130°C ↑9 °C/ min Hold 30min at 950°C
<b>Casting</b>			
<b>Cleaning of the casting</b>			
Sandblasting		Alumina oxide (Al <sub>2</sub> O <sub>3</sub> , 250 μm) under 6 atm pressure for 8 s	

casting of frameworks for metalceramic FPDs from dental alloys. The peculiarities of the technological process for production of fixed partial dentures from dental alloys by casting or pressing ceramics with 3D printed patterns are summarized in Table 6-5. The presented technological process provides high precision of the constructions and a 25% higher adhesion strength of porcelain coating compared to conventional casting with handmade wax models.

### 6.3. FIXED PARTIAL DENTURES, MANUFACTURED BY SELECTIVE LASER MELTING

During the SLM process, the details are produced directly from the virtual models, ensuring high accuracy and repeatability. To achieve a dense structure and high mechanical properties it is necessary optimal technological parameters to be used - laser power, speed and scanning strategy, layer thickness and distance between the individual traces.

Obtaining a dense structure in the workpiece volume without changing the thickness of the building layer and the distance between the individual traces can be achieved by varying the laser power and the scanning speed. It was established in the works of Wang J.H. et al. (2018) and of Grzesiak D. and Krawczyk M. (2015) that the optimum parameters of the SLM process that provide a dense structure and high mechanical properties of Co-Cr dental alloys are: laser power 160 W, scanning speed 1100 mm/s, and distance between the individual traces of 0.05 mm. The energy density calculated with these data is  $E=97 \text{ J/mm}^2$ , so in our work we consider this value as optimal.

*Table 6-7.*  
*Technological parameters of the SLM process in manufacturing of dental bridges.*

Parameter	N, W	V, mm/s	l <sub>c</sub> , mm	t <sub>c</sub> , mm	E, J/mm <sup>2</sup>
<i>Regime I of manufacturing of dental bridges</i>					
Volume border	100	500	0,13	0,03	51,3
Volume area	100	340	0,13	0,03	75,4
Volume offset hatch	95	400	0,13	0,03	60,9

The analysis and comparison with the technological parameters used for SLM of the bridge constructions (Regime 1, Table 6-7) showed that at all stages of layer formation the energy density was less than  $97 \text{ J/mm}^2$ , i.e., insufficient for formation of high density structure. In order to achieve the optimal energy density while maintaining all other parameters, it is necessary to increase the laser power, as it varies in the different stages of the layer manufacturing (Regime 2, Table 6-8). One more regime is proposed, in which the same technological parameters are used throughout the process (Regime 3, Table 6-8).

*Table 6-8*

*Algorithm, peculiarities and regimes in design of the virtual model and SLM process for manufacturing frameworks of FPDs.*

<b>Technological feature</b>	<b>Crown</b>	<b>Bridge</b>			
<b><i>Процес на 3D печат</i></b>					
Equipment	<i>SLM 125</i>				
Alloy	Co212-f ASTM F75				
Layer thickness	30 $\mu\text{m}$				
<b><i>Design of the virtual model</i></b>					
Position	Vertical axes of the teeth must be parallel to the printing direction Z-axes.				
Corrections of the dimensions	Increase with 0.15 mm along the three axes.				
<b><i>Technological regime of the SLM</i></b>					
<b>Parameter</b>	<b>N, W</b>	<b>V, mm/s</b>	<b>lc, mm</b>	<b>tc, mm</b>	<b>E, J/mm<sup>2</sup></b>
<b>Regime 2</b>					
Volume border	190	500	0,13	0,03	97,4
Volume area	130	340	0,13	0,03	98,0
Volume offset hatch	150	400	0,13	0,03	96,2
<b>Regime 3</b>					
Volume border	190	500	0,13	0,03	97,4
Volume area	190	500	0,13	0,03	97,4
Volume offset hatch	190	500	0,13	0,03	97,4
<b><i>Additional treatment</i></b>					
Sandblasting	<b>In manufacturing of frameworks for metalceramic FPDs: NOT APPLICABLE</b>				

The algorithm, features in designing a virtual model, and proposed optimal technological regimes of the SLM process for fabricating dental constructions with dense structure, high accuracy and mechanical properties are summarized in Table 6-8. In order to

ensure high adhesion strength of the porcelain coating in metalceramic FPDs, the SLM frameworks *should not be sandblasted*. It is proposed for the first time in our study in manufacturing frameworks for metalceramic dental prostheses *the sandblasting operation to be eliminated*, which will further reduce the time and the means of production.

#### **6.4. APPLICATION OF ADDITIVE TECHNOLOGIES IN THE TREATMENT PROCESS WITH FIXED PARTIAL DENTURES**

The present work has demonstrated the undisputed advantages of the additive technologies in production of dental constructions. They can be used at all stages of the manufacturing process - from the working model to the finished ceramic or metalceramic prosthesis.

Depending on the equipment, used for taking the impressions - intraoral or extraoral (laboratory) scanner, the treatment of the patients is carried out in a fully or partially digitized plan which: 1) increases the quality of the dental constructions; 2) reduces the procedure time and 3) increases the quality of the health service.

At the Faculty of Dental Medicine (FDM) - Varna, the additive technologies are implemented in the practice for solving clinical cases in the treatment of patients with FPDs. The topics for the application of the AT are included in the training programs of the specialities Dental Medicine and Dental Technicians of the FDM and Medical College at Medical University of Varna.

The presented clinical case convincingly demonstrates that the additive technologies are successful and promising alternative to conventional in the manufacture of fixed partial dentures.

## CONCLUSION

In recent decades, the development of new materials and new production technologies has been carried out under exponential law, and these two processes have constantly exchanged their leading role. According to the rules of the modern market economy, equipment manufacturers try to implement it as quickly as possible in the real production, which is further enhanced by the broad introduction of digitization, computerization and globalization. Under these conditions, it is necessary to continuously carry out research in order to ensure efficient and rapid production of details with high accuracy and quality through the new technological processes.

The present work explores the peculiarities of a new group technologies – additive technologies that arose in the 1980s. With its undisputed advantages - a wide variety of technological processes, application of nearly the whole range of materials, easy control and management as part of the CAD-CAM systems and almost waste-free production, it is a promising and successful alternative to conventional technologies in the production of traditional and personalized constructions with complex shapes in dental and general medicine.

The properties of two of the main groups of dental materials - dental polymers and dental alloys produced using different additive technologies - from stereolithography to selective laser melting, were studied using standard and new methodologies and approaches. It has been found that this type of technologies provides higher accuracy, mechanical and tribo-corrosion properties. The main role of the optical properties of dental polymers for manufacturing of high precision details through the stereolithography process is justified. It has been found for the first time, that the increased surface roughness of dental alloys, fabricated using additive technologies, is an advantage in production of metalceramic fixed partial dentures as it results in a higher adhesion strength of the porcelain coating.

On the basis of the results obtained, correction coefficients and algorithms for design of virtual models were proposed as well as a range of improved technologies for production of high-quality

temporary and permanent fixed partial dentures using additive technologies were developed.

The high precision and properties of the dental materials and constructions, produced by additive technologies, which have been demonstrated in the work, are not only a good prerequisite but also a basis for the successful implementation of the additive technologies into the dental laboratories and dental clinics.

## CONTRIBUTIONS

### 1. Scientific contricbutions

#### *New theory*

1.1. For the first time, the primary and decisive role of the optical properties of dental polymers for production of high precision constructions by stereolithography process is justified.

1.2. For the first time, it has been established that the increased roughness of dental alloys, fabricated using additive technologies, is an advantage in manufacturing of metalceramic fixed partial dentures, because it results in higher adhesion strength of the porcelain coating.

#### *New methodology*

1.3. A new methodology and device for investigation bending strength of dental alloys were developed using the most loaded four-part bridge constructions from 1-st premolar to 2-nd molar and providing application of the load closest to the actual.

1.4. A new non-destructive *in-vitro* method for evaluation the fitting accuracy of dental constructions such as inlays, onlays, crowns and bridges was developed. It ensures possibility for measuring the gap between the prepared teeth and the constructions in all directions with one order higher accuracy (0.01 mm) than that of the existing methods.

1.5. An improved criterion was developed for evaluation the fracture mode of porcelain coating on dental alloys.

## ***New technology***

1.6. A range of improved technologies has been developed and proposed for production of high-quality temporary and permanent fixed partial dentures using additive technologies.

## **2. Scientific-applied contributions**

### ***Original contributions***

2.1. It has been found that except the thickness of the building layer and the position of the workpiece relative to the printing direction, two more factors affect the surface roughness of dental polymers produced by stereolithography - the optical properties of the monomers used and the formation of the surfaces at the beginning or end of the process.

2.2. For the first time, adhesion strength of ceramic and composite coatings was investigated by tensile test of dental alloys. The advantage of the proposed approach compared to ISO Standard 9693-1: 2012 is the ability to determine the adhesion strength of a coating not only of porcelain but also of composite.

2.3. For the first time the elasticity modules of dental porcelain and composite are determined in tensile tests (63-72 GPa and 8.5 GPa respectively).

2.4. Fracture modes of porcelain and composite coatings on Co-Cr dental alloys, produced by casting with 3D printed patterns and SLM, have been established and proven. While the failure mode of the composite coating is adhesive, the fracture of the porcelain coating is of mixed mode, which, depending on the adhesion strength, can be mixed/adhesive in the cast alloy or mixed/cohesive in the SLM alloy.

2.5. For the first time the bending strength of the most loaded four-part dental bridges from 1-st premolar to 2-nd molar, fabricated of Co-Cr alloys by casting with 3D printed patterns and SLM, has been investigated by a newly developed methodology.

2.6. Different fracture modes of Co-Cr dental alloys, produced by casting and SLM, have been established: the SLM bridge constructions are destroyed suddenly without origination and propagation of crack, characteristic of the cast specimens. Fracture

mechanisms of the alloys produced by the two technologies are proposed.

2.7. It is found that the loads for crack initiation in bending of Co-Cr bridges, cast by conventional technology or with 3D printed patterns (9.820 kN and 10.171 kN, respectively), are close to the fracture load of the SLM dental bridges of *Co212-f* alloy (9.255 kN).

2.8. It has been established that in bending the distribution and magnitude of the normal and equivalent stresses as well as deformations are very similar in Co-Cr alloys, produced by the three technologies – conventional casting, casting with 3D printed patterns and SLM.

2.9. For the first time a study of the tribio-corrosive behavior in artificial saliva (*Fusayama-Meyer*) of Co-Cr dental alloy *Co212-f*, manufactured by SLM, is performed. It is established that the SLM alloy is more resistant to both corrosion and wear compared to the *Biosil-F* cast alloy and is characterized by a different type of surface wear.

### ***Confirmatory contributions***

2.10. It has been experimentally proven that the processes of stereolithography and multi-jet printing provide high accuracy and low roughness of dental polymers as compared to the fused deposition modeling.

2.11. It has been experimentally confirmed that the fitting accuracy of fixed partial dentures from dental polymers and dental alloys, manufactured using additive technologies, is higher than conventional fabricating, as the gap between the abutment teeth and the crown-retainers is within the clinically acceptable range but is unevenly distributed.

2.12. It has been experimentally proven that the surface roughness of 3D printed dental polymers and dental alloys, cast with 3D printed patterns or made by selective laser melting, is 2-4 times higher than that of conventionally manufactured materials.

2.13. It has been confirmed that the microstructure of Co-Cr bridge constructions, cast with 3D printed models is a typical cast structure - inhomogeneous with dendritic morphology. Is is

characterized with  $\gamma$ -phase in dendrites and small amounts of  $\varepsilon$ -phase, and in the interdendritic regions - with microeutectic and primary carbides of the type  $(\text{Cr},\text{Mo})_{23}\text{C}_6$ . The microeutectic consists of  $\gamma$ -solid solution and intermetallic inclusions of  $\text{Co}_5(\text{Cr},\text{Mo})_3\text{Si}_2$  type.

2.14. It has been confirmed that the macrostructure of the SLM Co-Cr alloy *Co212-f* is characterized by clearly visible layers and boundaries between them, while the microstructure is fine and homogeneous with dendritic morphology and  $\gamma$ -phase in dendrites, presence of higher quantity  $\varepsilon$ -phase and carbides of the mixed type  $\text{M}_{23}\text{C}_6$ .

2.15. The higher mechanical properties - hardness (356 HV0.1 - 407 HV0.1) and yield strength (720 MPa) of the SLM *Co212-f* alloy as compared to cast *Biosil-F* alloy (326 HV0.1 – 343 HV0.1 and 410 MPa respectively) are confirmed.

2.16. It is found that the hardness of the two alloys - the SLM *Co212-f* and the cast *Biosil-F* changed in a different way after firing a porcelain coating on them: the hardness of the SLM samples decreased to 36.5 HRC and that of the cast increased to 39.8 HRC.

### **3. Applied contributions**

#### ***Original contributions***

3.1. The terms "tehnologii za posloino izgrajdane" [in Bulgarian] and "posloino izgradeni materialii" [in Bulgarian] are proposed for wide usage.

3.2. For the first time by multi-criteria optimization the regimes of 3D printing of cast patterns were established, providing higher adhesion strength of porcelain coating to cast dental alloy.

3.3. For the first time correction coefficients and algorithms for design of the virtual models were proposed, which to ensure high precision of temporary and permanent fixed partial dentures in production by additive technologies.

## PUBLICATIONS ON DISERTACION

### 1. Individual publications

#### 1.1. Publications in scientific journals, indexed in the world databases - Thomson Reuters, Scopus, Google Scholar etc.

##### *Book chapter*

1.1.1. **Dikova T.** *Properties of Co-Cr Dental Alloys Fabricated Using Additive Technologies.* In Biomaterials in Regenerative Medicine, Prof. Leszek A. Dobrzański (Ed.), 2018. InTech, DOI: 10.5772/intechopen.69718.

##### *Papers*

1.1.2. **Dikova T,** *Bending fracture of Co-Cr dental bridges, produced by additive technologies: experimental investigation.* Procedia Structural Integrity, 2018 Dec; 13:461-468.

1.1.3. **Dikova T,** *Production of high quality temporary crowns and bridges by stereolithography,* Scripta Scientifica Medicinae Dentalis. 2019.

#### 1.2. Papers in scientific journals and conferences' proceedings

1.2.1. **Дикова Ц.,** *Фактори, оказващи влияние върху качеството на Co-Cr денални сплави, отлети с 3D принтирани модели.* [in Bulgarian] Foundry 2017;1(1):58-62.

1.2.2. **Дикова Ц.,** *Изследване плътността на денални мостови конструкции, изработени чрез избирателно стопяване с лазер.* [in Bulgarian] Сборник на МНК "Industry 4,0", 13-16.12.2017, Боровец, България, НТСМ. 2017 дек;1(1):149-152.

### 2. Publications in scientific journals, indexed in the world databases – Thomson Reuters, Scopus, Google Scholar etc.

2.1. **Dikova T,** Dzhendov D, Simov M, Katreva-Bozukova I, Angelova S, Pavlova D, Abadzhiev M, Tonchev T. *Modern trends in the development of the technologies for production of dental constructions.* J of IMAB. 2015 Oct-Dec;21(4):974-981.

2.2. **Dikova Ts.,** Dzh. Dzhendov, M. Simov, *Microstructure and Hardness of Fixed Dental Prostheses Manufactured by Additive Technologies,* Journal of Achievements in Mechanical and Materials Engineering, 2015 Aug;71(2):60-69;

2.3. **Dikova T,** Dzhendov D, Katreva I, Pavlova D, Simov M, Angelova S, Abadzhiev M, Tonchev T. *Possibilities of 3D printer Rapidshape D30 for*

*manufacturing of cubic samples*. Scripta Scientifica Medicinae Dentalis. 2016;2(1):9-15;

**2.4. Dikova Ts.**, Dzhendov D., Katreva I., Pavlova D. *Accuracy of polymeric dental bridges manufactured by stereolithography*. Archives of Materials Science and Engineering. 2016; 78(1):29-36;

**2.5. Vasilev T, T Dikova**, D Dzhendov, E Ivanova, *Simulations of Cast and Selective Laser Melted Dental Bridges with Chewing Load*, Scripta Scientifica Medicinae Dentalis. 2016;2(2):7-11.

**2.6. Dikova T**, Vasilev T, D Dzhendov, E Ivanova, *Investigation the fitting accuracy of cast and SLM Co-Cr dental bridges using CAD software*, J of IMAB. 2017 Jul-Sep;23(3):1688-1696;

**2.7. Dikova T.**, Dzhendov D., Katreva I., Tonchev T. *Study the precision of fixed partial dentures of Co-Cr alloys cast over 3D printed prototypes*. Archives of Materials Science and Engineering. 2018 March;90(1):25-32;

**2.8. Katreva I, Dikova T**, Tonchev T. *3D printing – an alternative of conventional crown fabrication: a case report*. J of IMAB. 2018 Apr 1;24(2):2048-54.

**2.9. Дикова Ц.**, Долгов Н., Василев Т., Катрева И. *Адгезионная прочность керамических покрытий стоматологического Ni–Cr-сплава, полученного литьем с применением 3D-печати*. [in Russian] Деформация и разрушение материалов. 2018 Сеп.;9:33-39;

**2.10. Dikova T.**, Vasilev T. *Bending fracture of Co-Cr dental bridges, produced by additive technologies: simulation analysis and test*. Engineering Fracture Mechanics.

**2.11. Dikova T.**, Vasilev T., Dolgov N. *Failure of ceramic coatings on cast and selective laser melted Co-C r dental alloys under tensile test: Experiment and finite element analysis*. Engineering Failure Analysis.

### **3. Papers in scientific journals and conferences' proceedings**

**3.1. Джендов Д., Павлова Д., Симов М., Маринов Н., Софронов Я., Дикова Ц.,** Тодоров Г., Кальчев Я. *Геометрична точност на неснемаеми мостови конструкции, изработени посредством адитивни технологии*, [in Bulgarian] Сборник на 8 МНК за млади учени “Technical Science and Industrial Management”, 15-16.09.2014, Варна, България, НТСМ. 2014;1:13-17;

**3.2. Дикова Ц.**, Джендов Д., Симов М., Павлова Д. *Дефекти на дентални мостове, изработени чрез леене и послойно лазерно*

стояване, [in Bulgarian] Научни известия, НТСМ, 2015 април;3(166):82-86;

**3.3.** Dolgov N.A., *Dikova Ts.*, Dzhendov D., Pavlova D., Simov M. *Mechanical Properties of Dental Co-Cr Alloys Fabricated via Casting and Selective Laser Melting*. Int. Journal “Materials Science. Non-Equilibrium Phase Transformations”. 2016;2(3):3-7;

**3.4.** Atapek H., *Dikova Ts.*, Aktaş G., Polat Ş., Dzhendov Dzh., Pavlova D. *Tribo-Corrosion Behavior of Cast and Selective Laser Melted Co-Cr Alloy for Dental Applications*, Int. Journal “Machines, Technologies, Materials”. 2016;10(12):61-64;

**3.5.** *Dikova T.*, Dzhendov D., Katreva I., Pavlova D., Tonchev T., Doychinova M. *Geometry and Surface Roughness of Polymeric Samples Produced by Stereolithography*, Int. Journal “Machines, Technologies, Materials”. 2017;11(4):201-205;

**3.6.** *Dikova T.*, Dolgov N., Dzhendov D., Simov M. *Adhesion strength evaluation of ceramic coatings on cast and selective laser melted Co-Cr dental alloys using tensile specimens*, Int. Journal “Materials Science. Non-Equilibrium Phase Transformations”. 2017;3(2):49-52;

**3.7.** Василев Т., *Дикова Ц.*, Джендов Д., Иванова Е. *Нова методика за измерване на хлабини на дентални мостови конструкции с използване на CAD софтуер*, [in Bulgarian] Сборник на 3-та МНК “Materials Science. Nonequilibrium Phase Transformations”, 11-14.09.2017, Варна, България, НТСМ. 2017;1(1):88-91;

**3.8.** Василев Т., *Дикова Ц.*, Иванова Е. *Методика за проектиране на приспособление за огъване на четиричленни дентални мостове*. [in Bulgarian] Сборник на МНК “Industry 4,0”, 13-16.12.2017, Боровец, България, НТСМ. 2017 дек;1(1):25-128.